

Incommensurate magnetic states induced by ordering competition in $\text{Ba}_{1-x}\text{Na}_x\text{Fe}_2\text{As}_2$

Jing Wang*

Department of Physics, Tianjin University, Tianjin 300072, P.R. China

(Dated: December 22, 2024)

Quantum criticality nearby certain magnetic phase transition beneath the superconducting dome of $\text{Ba}_{1-x}\text{Na}_x\text{Fe}_2\text{As}_2$ is attentively studied by virtue of a phenomenological theory in conjunction with renormalization group approach. We report that ordering competition between magnetic and superconducting fluctuations is capable of coaxing incommensurate (IC) magnetic states to experience distinct fates depending upon their spin configurations. C_2 -symmetry IC magnetic stripe with perpendicular magnetic helix dominates over other C_2 -symmetry magnetic competitors and hints to a potential candidate for the unknown C_2 -symmetry magnetic state. Amongst C_4 -symmetry IC magnetic phases, IC charge spin density wave is substantiated to be the winner shedding light on the significant intertwining of charge and spin degrees of freedom. Meanwhile, ferocious fluctuations render a sharp fall of superfluid density alongside with dip of critical temperature as well as intriguing behavior of London penetration depth.

PACS numbers: 74.70.-b, 74.20.De, 74.25.Dw, 74.62.-c

Introduction - Last dozen years have witnessed considerably intense research devoted to iron pnictides of BaFe_2As_2 family [1–13], whose phase diagrams are ubiquitously born out of both superconducting (SC) and diverse kinds of magnetic orders mediated by quantum phase transitions (QPTs) [14]. Notwithstanding magnetism is an antagonistic state versus superconductivity, they compete and collaborate other than coexist with each other [12, 13, 15]. This accordingly poses a substantial challenge what is the connection between magnetic and SC states providing a crucial ingredient to glue Cooper pairing [12, 13]. In the light of abundant magnetic states in BaFe_2As_2 [4–11], one of the most imperative and realistic quests of understanding this very compound, prior to exploring the ultimate SC nature, is how to unambiguously identify concrete configurations of magnetic states around QPTs in that different states are associated with distinguished fluctuations which play a pivotal role in establishing its phase diagram.

Instead of global scenario, the focus of this paper is put on pinning down specific magnetic states that reside close to magnetic QPTs in the phase diagram of $\text{Ba}_{1-x}\text{Na}_x\text{Fe}_2\text{As}_2$ [4, 5, 8–10]. This compound provides a versatile platform to investigate ordering-competition impacts on stabilities of magnetic states and relations with SC state. On one hand, it hosts a rather rich phase diagram with typical doping-tuned magnetic QPTs compared to other BaFe_2As_2 systems. It is of unique interest to asseverate there exists an elusive C_2 -symmetry (C_2) magnetic phase in Na-doped system reported recently by Wang *et al.* [8], which is hitherto enigmatic and remains an open topic. On the other, three commensurate plus twelve IC sorts of magnetic states all might be possible candidates inhabiting in its phase diagram [5, 6, 16–19]. Due to their own peculiarities, these distinct states conventionally bring forward various outcomes. Questions are naturally raised: which one is the prime C_4 -symmetry (C_4) magnetic order in the shadow of some QPT and

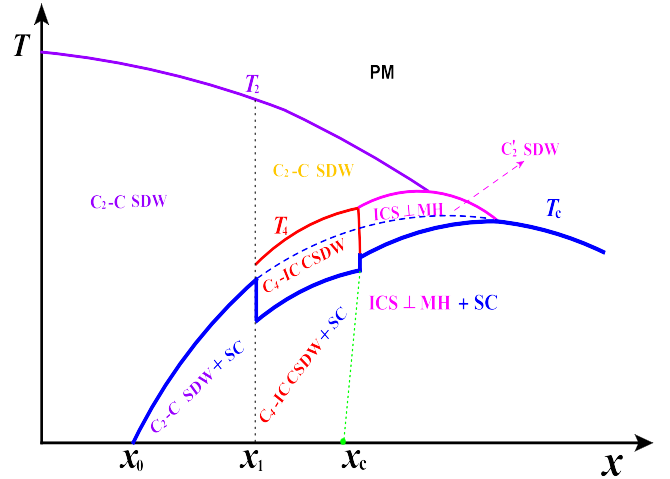


FIG. 1: (Color online) Schematic $x - T$ phase diagram of $\text{Ba}_{1-x}\text{Na}_x\text{Fe}_2\text{As}_2$ in the vicinity of vital magnetic quantum critical point (QCP) located at x_c . PM, SDW, and SC are shortened notations for paramagnetism, spin density wave (SDW), and superconductivity with $T_{2,4}$ and T_c denoting the critical temperatures from PM to $C_{2,4}$ SDW and non-SC to SC, respectively. Ordering competition bears out that C_2 ICS \perp MH state is a good candidate for the cryptic C_2 magnetic state (C_2' SDW) and the leading C_4 SDW close by the QCP is preferable to be IC CSDW, which are manifestly substantiated and supported by the combination of Table I and Fig. 2. Instead C_2 IC SDW can either be C_2 ICS, DPMH, or MH state as addressed in Supplementary Material (SM) [21] (the abbreviations of states hereby are consistent with Table I's).

what is the optimal state characterizing the mystic C_2 magnetic state. We are going to make a response taking advantage of a phenomenological theory together with the Wilsonian renormalization group (RG) [20]. Answers are of notable help to deeply understand the phase diagram and even offer instructive insights into pairing mechanism. Fig. 1 schematically illustrates our central

results driven by ordering competition.

Effective theory and RG analysis - Fermi surfaces of BaFe₂As₂ compounds under a three-band model consist of one hole pocket at the center of Brillouin zone $\mathbf{Q}_\Gamma = (0, 0)$ and two electron pockets centered at two fixed momenta $\mathbf{Q}_X = (\pi, 0)$ and $\mathbf{Q}_Y = (0, \pi)$ [13, 22–24]. For microscopical consideration, both magnetic and SC states are rooted in interactions among excited quasiparticles from these Fermi pockets [13, 16, 17, 22–25]. Concretely, a magnetic state is composed of two basic magnetic order parameters \mathbf{M}_X and \mathbf{M}_Y , which are designated by $\mathbf{M}_j = \sum_{\mathbf{k}} c_{\Gamma, \mathbf{k}\alpha}^\dagger \vec{\sigma}_{\alpha\beta} c_{j, \mathbf{k}+\mathbf{Q}_j\beta}$ with $j = X, Y$ [23–27]. To involve IC magnetic states, ordering vectors are afterwards distributed as $\mathbf{Q}_X = (\pi - \delta, 0)$ and $\mathbf{Q}_Y = (0, \pi - \delta)$ with δ being a small correction for generic wavevectors. This indicates that the magnetic order parameters are regarded as a complex quantity $M_{\mathbf{Q}_{X,Y}} \neq M_{\mathbf{Q}_{X,Y}}^* \equiv M_{-\mathbf{Q}_{X,Y}}$, which is in striking contrast to the commensurate case with $\delta = 0$ and $M_{\mathbf{Q}_{1,2}}^* = M_{\mathbf{Q}_{1,2}}$ [16, 17, 19].

We begin with the extended Landau-Ginzburg free energy after integrating out the fermionic ingredients [16,

17, 19, 28, 29]

$$f = \alpha(|\mathbf{M}_X|^2 + |\mathbf{M}_Y|^2) + \frac{\beta_2}{2}(|\mathbf{M}_X|^2 + |\mathbf{M}_Y|^2)^2 + \frac{\beta_1 - \beta_2}{2}(|\mathbf{M}_X^2|^2 + |\mathbf{M}_Y^2|^2) + (g_1 - \beta_2)|\mathbf{M}_X|^2|\mathbf{M}_Y|^2 + \frac{g_2}{2}(|\mathbf{M}_X \cdot \mathbf{M}_Y|^2 + |\mathbf{M}_X \cdot \mathbf{M}_Y^*|^2), \quad (1)$$

with α , $\beta_{1,2}$, and $g_{1,2}$ being fundamental structure parameters. It deserves pointing out that the QCP at x_1 in Fig. 1 associated with commensurate states was studied previously [16–18]. In order to judge and determine the unknown C_2 and C_4 IC SDWs, we hereafter concentrate on the magnetic QPT denoted by x_c in Fig. 1. After designating $\mathbf{M}_X \equiv M_X \cos \theta \mathbf{n}_X$ and $\mathbf{M}_Y \equiv M_Y \sin \theta \mathbf{n}_Y$, where $\theta \in (0, \pi/2)$ and $|\mathbf{n}_{X,Y}|^2 = 1$ specify the spin configurations of magnetic states, we go beyond mean-field level and construct a phenomenological effective field theory [16, 23], which captures main information of ordering competition including both $C_{2,4}$ -symmetric IC magnetic and SC fluctuations [18, 30–32] and takes the form

$$\mathcal{L}_{\text{eff}} = \left[\frac{1}{2}(\partial_\mu M_X / \mathcal{C})^2 + \alpha_X M_X^2 + \frac{\beta_X}{2} M_X^4 \right] + \left[\frac{1}{2}(\partial_\mu M_Y / \mathcal{S})^2 + \alpha_Y M_Y^2 + \frac{\beta_Y}{2} M_Y^4 \right] + \left[-\frac{1}{4}(\partial_\mu A_\nu - \partial_\nu A_\mu)^2 + \frac{\alpha_A}{2} A^2 \right] + \left[\frac{1}{2}(\partial_\mu h)^2 + a_h h^2 + \frac{\beta_h}{2} h^4 + \gamma_h h^3 \right] + \alpha_{XY} M_X M_Y + \gamma_{XYh} M_X M_Y h + \gamma_{X^2h} M_X^2 h + \gamma_{Y^2h} M_Y^2 h + \gamma_{hA^2} h A^2 + \lambda_{XY} M_X^2 M_Y^2 + \lambda_{Xh} M_X^2 h^2 + \lambda_{Yh} M_Y^2 h^2 + \lambda_{XYh} M_X M_Y h^2 + \lambda_{hA} h^2 A^2, \quad (2)$$

with $\mathcal{C} \equiv 1/|\mathbf{n}_X \cos \theta|^2$ and $\mathcal{S} \equiv 1/|\mathbf{n}_Y \sin \theta|^2$. The detailed derivations of this effective theory are presented in SM [21]. $M_{X,Y}$ point to magnetic fluctuations and h, A are auxiliary fields to absorb SC fluctuations. We here dub factors in (2) such as α_X etc. the effective parameters to prevent their being confused with fundamental parameters appearing in Eq. (1). Two series of parameters are bridged by virtue of Eqs. (11)-(19).

To proceed, we compute one-loop corrections to all effective parameters in Eq. (2) and derive the corresponding RG evolutions within Wilsonian RG framework [18, 20, 32] via integrating out the fast fields in the momentum shell $e^{-l}\Lambda < k < \Lambda$ with the running scale $l > 0$. Since the fundamental parameters defined in Eq. (1) dictate the physical properties, it heralds undeviatingly that a pillar of task consists in refining their flow equations. To this end, we resort to the strategy in Refs. [18, 32]. Combining RG flows of effective parameters and connections with fundamental parameters (11)-(19) yields a set of coupled RG equations

$$\frac{d\mathcal{X}_i}{dl} = \sum_j \mathcal{F}_{ij} \mathcal{X}_j, \quad (3)$$

with $\mathcal{X}_{i/j}$ serving as the fundamental parameters [33] and \mathcal{F}_{ij} standing for evolution coefficients as a function of $\mathcal{X}_{i/j}$. It necessitates bearing in mind that the coupled RG evolutions hinge heavily upon the spin configurations of magnetic fluctuations, namely the relationships between $|\mathbf{n}_X^2|^2$, $|\mathbf{n}_X|^4$, $|\mathbf{n}_Y^2|^2$, and $|\mathbf{n}_Y|^4$, which give rise to seven independent classes of RG evolutions. The details of Eq. (3) are stored completely in SM [21].

Fates of IC magnetic states - With the help of energy-dependent flows of fundamental parameters, we are now in a suitable situation to study the stabilities of IC magnetic states triggered by some magnetic QCP. As to BaFe₂As₂ compounds, many experimental efforts [4–11] corroborate that magnetism occupies major space of phase diagram in terms of various states with distinguished symmetries and spin configurations. Especially, compound Ba_{1-x}Na_xFe₂As₂ [5, 8–10] harbors a complicated but fascinating phase diagram sketched in Fig. 1, indicating a string of magnetic states for both C_2 and C_4 symmetries are allowed with proper variations of temperature and doping. Besides three commensurate states, i.e., stripe spin density wave (SDW),

TABLE I: Collections of low-energy fates for IC magnetic states in $\text{Ba}_{1-x}\text{Na}_x\text{Fe}_2\text{As}_2$. The first line enumerates seven distinguished types of IC magnetic states and the second line shows stable constraints as functions of fundamental interaction parameters [19] as well as the third line presents the corresponding low-energy stabilities. Herein, \checkmark and \times stand for a stable state (i.e., the prevailing candidate by the side of the magnetic QCP) and an unstable state, respectively.

IC magnetic states	ICS	MH	ICS \perp MH	DPMH	IC CSDW	IC SVC	SWC
Stable constraints	$\beta_1 - \beta_2 < 0$ with $\frac{g_2}{ \beta_1 - \beta_2 } > 0$, $\frac{g_1 - \beta_2}{ \beta_1 - \beta_2 } > -1$ or $\frac{g_2}{ \beta_1 - \beta_2 } < 0$, $\frac{g_1 - \beta_2 - 0.9g_2}{ \beta_1 - \beta_2 } > -1$	$\beta_1 - \beta_2 > 0$ with $\frac{g_2}{ \beta_1 - \beta_2 } > 0$, $\frac{g_1 - \beta_2}{ \beta_1 - \beta_2 } > 0$ or $\frac{g_2}{ \beta_1 - \beta_2 } < 0$, $\frac{g_1 - \beta_2 - 0.9g_2}{ \beta_1 - \beta_2 } > -1$	$\beta_1 - \beta_2 > 0$, $\frac{g_2}{ \beta_1 - \beta_2 } > 2$, $\frac{g_1 - \beta_2}{ \beta_1 - \beta_2 } < 0$	$\beta_1 - \beta_2 > 0$, $\frac{g_2}{ \beta_1 - \beta_2 } < 0$, $\frac{g_1 - \beta_2 - 0.9g_2}{ \beta_1 - \beta_2 } < -1$	$\beta_1 - \beta_2 < 0$, $\frac{g_2}{ \beta_1 - \beta_2 } < 0$, or $\beta_1 - \beta_2 > 0$, $\frac{g_2}{ \beta_1 - \beta_2 } < -1$, $\frac{g_1 - \beta_2 - 0.9g_2}{ \beta_1 - \beta_2 } < -1$	$\beta_1 - \beta_2 < 0$, $\frac{g_2}{ \beta_1 - \beta_2 } > 0$, $\frac{g_1 - \beta_2}{ \beta_1 - \beta_2 } < -1$	$\beta_1 - \beta_2 > 0$, $0 < \frac{g_2}{ \beta_1 - \beta_2 } < 2$, $\frac{g_1 - \beta_2}{ \beta_1 - \beta_2 } < 0$
Fates of magnetic states	\times	\times	\checkmark	\times	\checkmark	\times	\times

charge spin density wave (CSDW), and spin vortex crystal (SVC) [16, 17, 34, 35], Christensen *et al.* [19] recently advocated that potential IC magnetic states are clustered into nine inequivalent breeds. What is more, seven of them can be realized with confined parameters of mean-field free energy in the phase diagram [19], which cover four kinds of C_2 IC cases involving C_2 IC stripe (ICS), C_2 magnetic helix (MH), C_2 IC magnetic stripe with perpendicular magnetic helix (ICS \perp MH), and C_2 double parallel magnetic helix (DPMH), as well as three distinct C_4 IC situations consisting of C_4 IC CSDW, C_4 IC SVC, and C_4 IC spin-whirl crystal (SWC) along with the stable constraints catalogued point-to-point in the second line of Table I.

Despite of an underlying antagonist against SC state, magnetism is assumed to be of intimate relevance to superconductivity as they are closely adjacent to each other or even coexist near the magnetic QPT. To be concrete, we concentrate on an especial point in Fig. 1, namely the QCP at $T = 0$ that separates C_2 and C_4 IC magnetic states labeled by x_c . Generally, the related magnetic fluctuations compete so furiously that are always responsible for physics in the shadow of QPT including quantum critical regime with higher temperatures [14, 23, 24]. Considering individualities of diverse states in spite of hosting common magnetic generalities come up with different consequences, we thereafter contemplate the magnetic states on both sides of this QPT.

As it concerns the issue on intricate relationship between magnetism and superconductivity, a hallmark of fathoming overall phase diagram is tantamount to pinpointing the specific construction of each magnetic state. As a corollary, it is an appropriate pointcut that one investigates how the ordering competition affects the magnetic state on the edge of the QCP by means of RG

flows (3) in collaboration with the stable magnetic criteria itemized in the second line of Table I. In order to be baldly relevant with schematic phase diagram, we adopt $T = T_0 e^{-l}$ with T_0 the initial temperature to measure the evolution variable [18, 32]. Performing numerical analysis not only bears witness to the crucial role of ordering competition but also sheds light on fates of all types of IC magnetic states. Fig. 2 exhibits the temperature (energy) dependence of correlated fundamental parameters, which carry the low-energy characteristics for both C_2 ICS \perp MH and C_4 IC CSDW. At the outset, we find that stable constraints for C_2 ICS \perp MH shown in Fig. 2(a) are well protected with the decrease of temperature. They are sabotaged by extremely strong fluctuations only until the magnetic QCP is sufficiently accessed at the collapsed temperature $T_{\text{col}} \sim 10^{-4}T_0$ (taking $T_0 = 100$ K for instance, $T_{\text{col}} \sim 10^{-2}$ K). This evidently signals that C_2 ICS \perp MH is of particular robustness withstanding ordering competition. In reminiscence of the unknown C_2 magnetic state, which locates at a little deviation from the magnetic QCP portrayed in Fig. 1, we are aware that C_2 ICS \perp MH is therefore deemed to be a reasonable candidate for this mysterious C_2 state that differs substantially from conventional C_2 stripe state. In addition, reading off Fig. 2(b) proposes firmly robust temperature-dependent constraints for C_4 IC CSDW. We then come to a conclusion that IC CSDW, like its commensurate counterpart [18], behaves dominantly compared to other types of IC C_4 magnetic states. This C_4 magnetic state is henceforth the most applicable choice in the left side of magnetic QCP x_c in Fig. 1, which compete, coexist, and cooperate with SC state. Furthermore, apart from the two applicable states including C_2 ICS \perp MH and C_4 IC CSDW, ordering competition surrounding by magnetic QCP is not in favour of all other types of IC magnetic

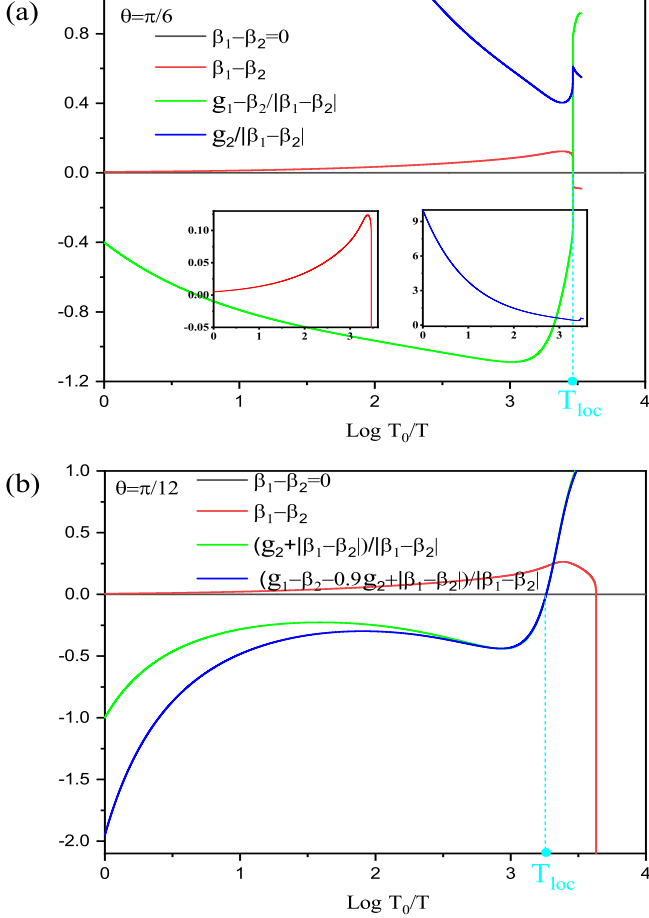


FIG. 2: (Color online) Temperature-dependent stable constraints of (a) C_2 ICS \perp MH and (b) C_4 IC CSDW under representative starting values of interaction parameters (the basic results are insensitive to initial values of parameters). T_{col} labels the very temperature at which the corresponding stable constraints are jeopardized and collapsed. Insets: enlarged regions for $\beta_1 - \beta_2$ and $g_2/|\beta_1 - \beta_2|$.

states listed in Table I. In terminological language, given these states are prone to easily feel plus efficiently receive the fluctuation corrections even far away from a magnetic QCP, they are fairly sensitive and fragile to ordering competition, resulting in undeviating breakdown themselves as temperature is reduced. It broadly suggests that one is unable to solely fix the configuration of C_2 IC SDW above C_4 IC CSDW and C_2 ICS \perp MH as displayed in Fig. 1, which may either be C_2 ICS, C_2 DPMH, or C_2 MH. The details of verifying stabilities of IC magnetic states are provided in SM [21]. Last but not the least important, we deliver that, as for the region close enough to the QCP with $T < T_{\text{col}}$, ordering competition is so ferociously that any magnetic state cannot exist alone but instead there might be a coexistence of multiple IC magnetic states.

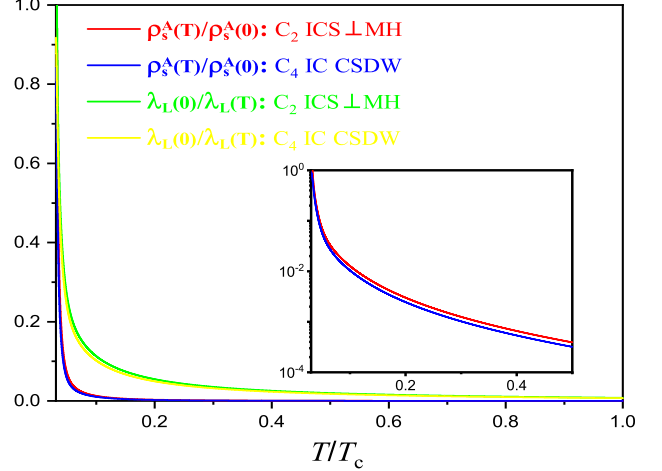


FIG. 3: (Color online) Superfluid density and London penetration depth as a function of temperature at $\theta = 6/\pi$ affected by C_2 ICS \perp MH and C_4 IC CSDW neighboring the magnetic QCP. T_c designates the related critical temperature without ordering competition (the essential features are insensitive to beginning values of interaction parameters). Inset: enlarged regions for ρ_s displaying difference between the two cases.

Superfluid density and London penetration depth - As magnetic states steadily compete and coexist with a SC order, it is of great temptation to examine how the superfluid density (ρ_s) and London penetration depth (λ_L) are influenced in the presence of ordering competition, which are of two particular importance implications. In principle, $\rho_s(T)$ can be evaluated as $\rho_s(T) = \rho_s^A(T) - \rho_n(T)$, where $\rho_s^A(T) \propto \alpha_A(T)$ stems from the mass of vector field \mathbf{A} that obey RG equations due to Anderson-Higgs mechanism [30] and $\rho_n(T)$ grasps the density of thermally excited normal (non-SC) fermionic quasiparticles (QPs), respectively. Approaching the QCP, ordering competition is dominant and thus the normal QPs effects can be neglected implying $\rho_s(T) \sim \rho_s^A(T)$. Fig. 3 clearly unveils that $\rho_s(T)$ is remarkably suppressed by the ordering competition [18, 36, 37]. Because critical temperature T_c is nominated by $\rho_s(T_c) = \rho_s^A(T_c) - \rho_n(T_c) = 0$, one can infer that it would be intensively reduced in the absence of $\rho_n(T)$. As explicitly delineated in the inset of Fig. 3, it is worth declaring that the drop of T_c caused by the C_4 IC CSDW is a little more than its C_2 ICS \perp MH's counterpart, which is also apparently exposed in Fig. 1. Albeit a slight splitting, principal tendencies are qualitatively compatible with recent experiments [6, 8, 10]. For qualitative discussions, we single out the s -wave gap symmetry as a toy and tentative substitute. In this respect, the London penetration depth is expressed as $\lambda_L(0)/\lambda_L(T) = \sqrt{\rho_s(T)}$ [38]. As a consequence, $\lambda_L(0)/\lambda_L(T)$ shares the analogous temperature-dependent trajectory with ρ_s under the im-

pect of ordering competition as depicted in Fig. 3. Although BaFe_2As_2 system possesses a more intricate gap structure [13], this primitive result might uncover parts of central ingredients that are in charge of λ_L 's property.

Summary - We study and discern the probable IC magnetic states induced by subtle ordering competition in the proximity of certain QPT below the SC dome of $\text{Ba}_{1-x}\text{Na}_x\text{Fe}_2\text{As}_2$. Specifically, we find that C_2 ICS \perp MH survives to be a good candidate for the obscure C_2 magnetic state and IC C_4 CSDW points to the reasonable IC state in the vicinity of the magnetic QPT. In addition, we address that superfluid density in tandem with critical temperature and London penetration depth manifest critical behaviors attesting to ordering competition around the QCP. The conclusions are qualitatively concomitant with recent experiments [6, 8, 10]. We expect our results are profitable to further understand the phase diagram of $\text{Ba}_{1-x}\text{Na}_x\text{Fe}_2\text{As}_2$ and explore the correspondence between SC and magnetic states in iron-based superconductors.

J.W. is partially supported by the National Natural Science Foundation of China under Grant No. 11504360 and highly grateful to Y. -J. Zhou for stimulating discussions on the June 11, 2020.

* E-mail address: jing.wang@tju.edu.cn

- [1] D. S. Inosov *et al.*, Nat. Phys. **6**, 178 (2010); J. Paglione and R. L. Greene, Nat. Phys. **6**, 645 (2010); P. Dai, J. Hu, and E. Dagotto, Nat. Phys. **8**, 709 (2012).
- [2] G. R. Stewart, Rev. Mod. Phys. **83**, 1589 (2011); E. Dagotto, Rev. Mod. Phys. **85**, 849 (2013); P. C. Dai, Rev. Mod. Phys. **87**, 855 (2015).
- [3] I. R. Fisher, L. Degiorgi, and Z. X. Shen, Rep. Prog. Phys. **74**, 124506 (2011); H.-H. Kuo *et al.*, Science **352**, 958 (2016); P. J. Hirschfeld, M. M. Korshunov, and I. I. Mazin, Rep. Prog. Phys. **74**, 124508 (2011).
- [4] M. G. Kim *et al.*, Phys. Rev. B **82**, 220503(R)(2010); S. Nandi *et al.*, Phys. Rev. Lett. **104**, 057006 (2010); E. Hassinger *et al.*, Phys. Rev. B **86**, 140502 (2012).
- [5] S. Avci *et al.*, Nat. Commun. **5**, 3845 (2014).
- [6] A. E. Böhmer, F. Hardy, L. Wang, T. Wolf, P. Schweiss, and C. Meingast, Nat. Commun. **6**, 7911 (2015).
- [7] J. M. Allred *et al.*, Phys. Rev. B **92**, 094515 (2015); E. Hassinger *et al.*, Phys. Rev. B **93**, 144401 (2016); J. M. Allred *et al.*, Nat. Phys. **12**, 493 (2016).
- [8] L. Wang, F. Hardy, A. E. Böhmer, T. Wolf, P. Schweiss, and C. Meingast, Phys. Rev. B **93**, 014514 (2016).
- [9] M. N. Gastiasoro, I. Eremin, R. M. Fernandes and B. M. Andersen, Nat. Commun. **8**, 14317 (2017).
- [10] M. Yi *et al.*, Phys. Rev. Lett. **121**, 127001 (2018); L. Wang *et al.*, Phys. Rev. B **97**, 224518 (2018).
- [11] E. I. Timmons *et al.*, Phys. Rev. B **99**, 054518 (2019); R. Prozorov *et al.*, NPJ Quantum Materials **4**, 34 (2019).
- [12] D. N. Basov and A. V. Chubukov, Nat. Phys. **7**, 272 (2011); R. M. Fernandes, A. V. Chubukov, and J. Schmalian, Nat. Phys. **10**, 97 (2014).
- [13] A. V. Chubukov, Annu. Rev. Condens. Matter Phys. **3**, 57 (2012); R. M. Fernandes and A. V. Chubukov, Rep. Prog. Phys. **80**, 014503 (2017); R. M. Fernandes, P. P. Orth, and J. Schmalian, Annu. Rev. Condens. Matter Phys. **10**, 133 (2019).
- [14] M. Vojta, Rep. Prog. Phys. **66**, 2069 (2003); S. Sachdev, Quantum Phase Transitions 1st ed. (Cambridge University Press, Cambridge, UK, 1999)
- [15] X. Chen, S. Maiti, R. M. Fernandes, and P. J. Hirschfeld, arXiv: 2004.13134v1 (2020).
- [16] R. M. Fernandes, A. V. Chubukov, J. Knolle, I. Eremin, and J. Schmalian, Phys. Rev. B **85**, 024534 (2012); R. M. Fernandes, S. A. Kivelson, and E. Berg, Phys. Rev. B **93**, 014511 (2016).
- [17] M. Hoyer, R. M. Fernandes, A. Levchenko, and J. Schmalian, Phys. Rev. B **93**, 144414 (2016).
- [18] J. Wang, G. -Z. Liu, D. V. Efremov, and J. van den Brink, Phys. Rev. B **95**, 024511, (2017).
- [19] M. H. Christensen, B. M. Andersen, and P. Kotetes, Phys. Rev. X **8**, 041022 (2018).
- [20] K. G. Wilson, Rev. Mod. Phys. **47** 773 (1975); J. Polchinski, arXiv: hep-th/9210046 (1992); R. Shankar, Rev. Mod. Phys. **66**, 129 (1994).
- [21] See the Supplementary Material.
- [22] I. Eremin and A. V. Chubukov, Phys. Rev. B **81**, 024511 (2010); J. Knolle, I. Eremin, A. V. Chubukov, and R. Moessner, Phys. Rev. B **81**, 140506(R) (2010).
- [23] R. M. Fernandes, S. Maiti, P. Wölfle, and A. V. Chubukov, Phys. Rev. Lett. **111**, 057001 (2013); A. Levchenko, M. G. Vavilov, M. Khodas, and A. V. Chubukov, Phys. Rev. Lett. **110**, 177003 (2013).
- [24] D. Chowdhury, B. Swingle, E. Berg, S. Sachdev, Phys. Rev. Lett. **111**, 157004 (2013).
- [25] A. V. Chubukov, D. V. Efremov, and I. Eremin, Phys. Rev. B **78**, 134512 (2008); S. Maiti and A. V. Chubukov, Phys. Rev. B **82**, 214515 (2010).
- [26] C. Fang, H. Yao, W.-F. Tsai, J. P. Hu, and S. A. Kivelson, Phys. Rev. B **77**, 224509 (2008); C. Xu, M. Muller, and S. Sachdev, Phys. Rev. B **78**, 020501(R) (2008).
- [27] R. M. Fernandes *et al.*, Phys. Rev. Lett. **105**, 157003 (2010).
- [28] H. J. Schulz, Phys. Rev. Lett. **64**, 1445 (1990).
- [29] M. H. Christensen, D. D. Scherer, P. Kotetes, and B. M. Andersen, Phys. Rev. B **96**, 014523 (2017).
- [30] B. I. Halperin, T. C. Lubensky, and S.-K. Ma, Phys. Rev. Lett. **32**, 292 (1974).
- [31] H. Kleinert and F. S. Nogueira, Nucl. Phys. B **651**, 361 (2003).
- [32] J. Wang and G.-Z. Liu, Phys. Rev. D **90**, 125015 (2014); J. Wang and G.-Z. Liu, Phys. Rev. B **92**, 184510 (2015).
- [33] Besides a , a_s , u_s , λ , β_1 , β_2 , g_1 , and g_2 appearing in the free energy (1), κ and $\lambda_{\Delta A}$ are two additional fundamental parameters as demonstrated in SM [21].
- [34] R. Yu, M. Yi, B. A. Frandsen, R. J. Birgeneau, and Q. Si, arXiv:1706.07087v1 (2017).
- [35] M. Klug, J. Kang, R. M. Fernandes, J. Schmalian, Phys. Rev. B **97**, 155130 (2018).
- [36] G.-Z. Liu, J.-R. Wang, and J. Wang, Phys. Rev. B **85**, 174525 (2012).
- [37] A. E. Koshelev, arXiv: 2005.14145 (2020).
- [38] E. Helfand and N. R. Werthamer, Phys. Rev. **147**, 288 (1966).

Supplementary Material: “Incommensurate magnetic states induced by ordering competition in $\text{Ba}_{1-x}\text{Na}_x\text{Fe}_2\text{As}_2$ ”

DERIVATIONS OF THE EFFECTIVE ACTION

We are going to take into account both magnetic and SC fluctuations in the vicinity of magnetic QCP shown in Fig. 1. To this end, the phenomenological effective action [16, 23] can be casted as

$$S = \int \mathcal{L} = \int \mathcal{L}_{\text{SDW}} + \int \mathcal{L}_{\text{SC}} + \int \mathcal{L}_{\text{SDW-SC}}, \quad (4)$$

where \mathcal{L}_{SDW} , \mathcal{L}_{SC} , and $\mathcal{L}_{\text{SDW-SC}}$ correspond to SDW, SC orders, and their interplay, respectively.

At first, we go to \mathcal{L}_{SDW} . Designating $\mathbf{M}_X \equiv M_X \cos \theta \mathbf{n}_X$ and $\mathbf{M}_Y \equiv M_Y \sin \theta \mathbf{n}_Y$, where $\theta \in (0, \pi/2)$ and $|\mathbf{n}_{X,Y}|^2 = 1$ describe the spin configurations of magnetic states, and inserting them into the free energy density (1) with adding the dynamical terms of magnetic order parameters give rise to [16, 18, 23, 28]

$$\begin{aligned} \mathcal{L}_{\text{SDW}} = & \left[|\mathbf{n}_X \cos \theta|^2 \frac{1}{2} (\partial_\mu M_X)^2 + \alpha (|\mathbf{n}_X|^2 \cos^2 \theta) M_X^2 \right] + \left[|\mathbf{n}_Y \sin \theta|^2 \frac{1}{2} (\partial_\mu M_Y)^2 + \alpha (|\mathbf{n}_Y|^2 \sin^2 \theta) M_Y^2 \right] \\ & + \frac{\beta_1 - \beta_2}{2} (|\mathbf{n}_X|^2 \cos^4 \theta M_X^4 + |\mathbf{n}_Y|^2 \sin^4 \theta M_Y^4) + \frac{\beta_2}{2} (|\mathbf{n}_X|^4 \cos^4 \theta M_X^4 + |\mathbf{n}_Y|^4 \sin^4 \theta M_Y^4) \\ & + g_1 |\mathbf{n}_X|^2 |\mathbf{n}_Y|^2 \cos^2 \theta \sin^2 \theta M_X^2 M_Y^2 + \frac{g_2}{2} \cos^2 \theta \sin^2 \theta (|\mathbf{n}_X \cdot \mathbf{n}_Y|^2 + |\mathbf{n}_X \cdot \mathbf{n}_Y^*|^2) M_X^2 M_Y^2. \end{aligned} \quad (5)$$

We next consider \mathcal{L}_{SC} . In order to obtain SC fluctuations in the ordered state, we bring out the the following contribution by employing the condition $\partial_\mu A_\mu = 0$ [30]

$$\mathcal{L}_{\text{SC}} = \left[\partial_\mu \Delta^\dagger \partial_\mu \Delta + a_s \Delta^2(k) + \frac{u_s}{2} \Delta^4(k) \right] + \left[-\frac{1}{4} (\partial_\mu A_\nu - \partial_\nu A_\mu)^2 + \frac{\alpha_A}{2} A^2 \right] + \lambda_{\Delta A} |\Delta|^2 A^2. \quad (6)$$

As the system enters into the SC ordered state around the SDW QCP, we need to expand the SC order parameter by introducing two new gapless fields

$$\Delta = V_0 + \frac{1}{\sqrt{2}}(h + i\eta), \quad \langle h \rangle = \langle \eta \rangle = 0, \quad V_0 \equiv \langle \Delta \rangle = \sqrt{\frac{-a_s}{u_s}}, \quad (7)$$

which help us to extract the potential fluctuation of SC order parameter [31], to make the \mathbf{A} massive after absorbing the gapless Goldstone particles,

Combing Eq. (6) and Eq. (7), we get after discarding the constant terms and choosing some transformation to make $\eta = 0$ due to the local gauge invariance [31],

$$\mathcal{L}_{\text{SC}} = \frac{1}{2} (\partial_\mu h)^2 - a_s h^2 + \frac{u_s}{8} h^4 + \frac{\sqrt{-2a_s u_s}}{2} h^3 - \frac{1}{4} (\partial_\mu A_\nu - \partial_\nu A_\mu)^2 + \frac{\alpha_A}{2} A^2 + \lambda_{\Delta A} \sqrt{\frac{-2a_s}{u_s}} h A^2 + \frac{\lambda_{\Delta A}}{2} h^2 A^2, \quad (8)$$

where the “mass” of field A being $\alpha_A \equiv \lambda_{\Delta A} \frac{-2a_s}{u_s}$.

At last, we introduce \mathcal{L}_{SC} . The interplay between SC and SDW order parameters can be written as [18],

$$\mathcal{L}_{\text{SDW-SC}} = \lambda (|\mathbf{M}_X|^2 + |\mathbf{M}_Y|^2) \Delta^2 + \kappa (|\mathbf{M}_X \cdot \mathbf{M}_Y| + |\mathbf{M}_X \cdot \mathbf{M}_Y^*|) \Delta^2. \quad (9)$$

Based on the information of \mathcal{L}_{SDW} and \mathcal{L}_{SC} , we are left with

$$\begin{aligned} \mathcal{L}_{\text{SDW-SC}} = & \frac{-a_s \lambda}{u_s} (|\mathbf{n}_X|^2 \cos^2 \theta M_X^2 + |\mathbf{n}_Y|^2 \sin^2 \theta M_Y^2) + \lambda \sqrt{\frac{-2a_s}{u_s}} (|\mathbf{n}_X|^2 \cos^2 \theta M_X^2 + |\mathbf{n}_Y|^2 \sin^2 \theta M_Y^2) h \\ & + \frac{\lambda}{2} (|\mathbf{n}_X|^2 \cos^2 \theta M_X^2 + |\mathbf{n}_Y|^2 \sin^2 \theta M_Y^2) h^2 + \frac{-a_s \kappa}{u_s} (|\cos \theta \sin \theta \mathbf{n}_X \cdot \mathbf{n}_Y| + |\cos \theta \sin \theta \mathbf{n}_X \cdot \mathbf{n}_Y^*|) M_X M_Y \\ & + \kappa \sqrt{\frac{-2a_s}{u_s}} (|\cos \theta \sin \theta \mathbf{n}_X \cdot \mathbf{n}_Y| + |\cos \theta \sin \theta \mathbf{n}_X \cdot \mathbf{n}_Y^*|) M_X M_Y h \\ & + \frac{\kappa}{2} (|\cos \theta \sin \theta \mathbf{n}_X \cdot \mathbf{n}_Y| + |\cos \theta \sin \theta \mathbf{n}_X \cdot \mathbf{n}_Y^*|) M_X M_Y h^2. \end{aligned} \quad (10)$$

To recapitulate, Eqs. (5), (6), and (10) constitute our effective theory (2). The effective parameters such as α_X etc. are connected with fundamental parameters appearing in Eq. (1) via following relationships

$$\alpha_h \equiv (-a_s), \beta_h \equiv \frac{u_s}{4}, \gamma_h \equiv \frac{\sqrt{-2a_s u_s}}{2}, \alpha_A \equiv \frac{-2\lambda_{\Delta A} a_s}{u_s}, \gamma_{hA^2} \equiv \lambda_{\Delta A} \sqrt{\frac{-2a_s}{u_s}}, \lambda_{hA} \equiv \frac{\lambda_{\Delta A}}{2}, \quad (11)$$

$$\alpha_X \equiv \left(a - \frac{\lambda a_s}{u_s}\right) (|\mathbf{n}_X|^2 \cos^2 \theta), \beta_X \equiv \beta_2 (|\mathbf{n}_X|^4 \cos^4 \theta) + (\beta_1 - \beta_2) (|\mathbf{n}_X^2|^2 \cos^4 \theta), \quad (12)$$

$$\alpha_Y \equiv \left(a - \frac{\lambda a_s}{u_s}\right) (|\mathbf{n}_Y|^2 \sin^2 \theta), \beta_Y \equiv \beta_2 (|\mathbf{n}_Y|^4 \sin^4 \theta) + (\beta_1 - \beta_2) (|\mathbf{n}_Y^2|^2 \sin^4 \theta), \quad (13)$$

$$\alpha_{XY} \equiv \frac{-a_s \kappa}{u_s} (|\cos \theta \sin \theta \mathbf{n}_X \cdot \mathbf{n}_Y| + |\cos \theta \sin \theta \mathbf{n}_X \cdot \mathbf{n}_Y^*|), \quad (14)$$

$$\gamma_{XYh} = \kappa \sqrt{\frac{-2a_s}{u_s}} (|\cos \theta \sin \theta \mathbf{n}_X \cdot \mathbf{n}_Y| + |\cos \theta \sin \theta \mathbf{n}_X \cdot \mathbf{n}_Y^*|), \quad (15)$$

$$\gamma_{X^2h} \equiv \lambda \sqrt{\frac{-2a_s}{u_s}} (|\mathbf{n}_X|^2 \cos^2 \theta), \gamma_{Y^2h} \equiv \lambda \sqrt{\frac{-2a_s}{u_s}} (|\mathbf{n}_Y|^2 \sin^2 \theta), \quad (16)$$

$$\lambda_{XY} \equiv g_1 \cos^2 \theta \sin^2 \theta (|\mathbf{n}_X|^2 |\mathbf{n}_Y|^2) + \frac{g_2}{2} \cos^2 \theta \sin^2 \theta (|\mathbf{n}_X \cdot \mathbf{n}_Y|^2 + |\mathbf{n}_X \cdot \mathbf{n}_Y^*|^2), \quad (17)$$

$$\lambda_{Xh} \equiv \frac{\lambda}{2} (|\mathbf{n}_X|^2 \cos^2 \theta), \lambda_{Yh} \equiv \frac{\lambda}{2} (|\mathbf{n}_Y|^2 \sin^2 \theta), \quad (18)$$

$$\lambda_{XYh} \equiv \frac{\kappa}{2} (|\cos \theta \sin \theta \mathbf{n}_X \cdot \mathbf{n}_Y| + |\cos \theta \sin \theta \mathbf{n}_X \cdot \mathbf{n}_Y^*|). \quad (19)$$

We hereby would like to emphasize that κ and $\lambda_{\Delta A}$ cannot be represented by original ones $a, a_s, u_s, \lambda, \beta_1, \beta_2, g_1$, and g_2 appearing in the free energy (1). This unambiguously substantiates the independence of κ and $\lambda_{\Delta A}$ and therefore comes up with two supplementary fundamental parameters.

COUPLED RG EQUATIONS OF FUNDAMENTAL INTERACTION PARAMETERS

After performing one-loop analysis of effective theory [18, 20, 32] via integrating out the fields in the momentum shell $e^{-l}\Lambda < k < \Lambda$ with $l > 0$ the running scale, we can derive flows of effective parameters in Eq. (2). Combining these equations and connections (11)-(19) [18, 32], the coupled RG equations for fundamental parameters can be derived.

Before going further, it is necessary to highlight that the fundamental parameters $g_{1,2}$ only appear in Eq. (17). This implies that they do not evolve independently. In this sense, it is hereafter convenient to introduce a pa-

rameter

$$\hat{g} \equiv g_1 \cos^2 \theta \sin^2 \theta (|\mathbf{n}_X|^2 |\mathbf{n}_Y|^2) + \frac{g_2}{2} \cos^2 \theta \sin^2 \theta (|\mathbf{n}_X \cdot \mathbf{n}_Y|^2 + |\mathbf{n}_X \cdot \mathbf{n}_Y^*|^2), \quad (20)$$

to describe the information of $g_{1,2}$.

After long but straightforward calculations [18, 32], we eventually obtain the coupled RG equations of all fundamental interaction parameters around the magnetic QCP, which include $\alpha, \beta_{1,2}, \hat{g}$ and κ specifying the characters of spin configurations as well as $a_s, u_s, \lambda_{\Delta A}$ stemming from SC fluctuations. These coupled RG evolutions are closely dependent upon the spin configurations of magnetic fluctuations, namely the relationships between $|\mathbf{n}_X^2|^2, |\mathbf{n}_X|^4, |\mathbf{n}_Y^2|^2, |\mathbf{n}_Y|^4$, which are divided into two main sorts of situations.

For type-I case, at which $|\mathbf{n}_X^2|^2 \neq |\mathbf{n}_X|^4$ and $|\mathbf{n}_Y^2|^2 = |\mathbf{n}_Y|^4$ or $|\mathbf{n}_X^2|^2 = |\mathbf{n}_X|^4$ and $|\mathbf{n}_Y^2|^2 \neq |\mathbf{n}_Y|^4$, both β_1 and β_2 flow independently and thus the coupled evolutions are written as

$$\begin{aligned} \frac{da_s}{dl} = & 2a_s - \frac{1}{4\pi^2} \left\{ \frac{9a_s u_s (1 + 4a_s)}{2} + \frac{2S\mathcal{E}_1^2 a_s \lambda^2}{u_s} [1 - 4S\mathcal{E}_1 (a - \frac{\lambda a_s}{u_s})] + \frac{2C\mathcal{D}_1^2 a_s \lambda^2}{u_s} [1 - 4C\mathcal{D}_1 (a - \frac{\lambda a_s}{u_s})] \right. \\ & + \frac{32a_s \lambda_{\Delta A}^2}{3u_s} (1 + \frac{4\lambda_{\Delta A} a_s}{u_s}) + \frac{(S\mathcal{E}_1 + C\mathcal{D}_1)\lambda}{2} + \frac{3u_s (1 + 2a_s)}{4} - (a - \frac{\lambda a_s}{u_s}) (\mathcal{E}_1^2 S^2 + \mathcal{D}_1^2 C^2) \lambda \\ & \left. + \lambda_{\Delta A} (1 + \frac{2\lambda_{\Delta A} a_s}{u_s}) + \frac{CS\mathcal{F}^2 a_s \kappa^2}{4u_s} [1 - 2(C\mathcal{D}_1 + S\mathcal{E}_1)(a - \frac{\lambda a_s}{u_s})] \right\}, \quad (21) \end{aligned}$$

$$\begin{aligned} \frac{da}{dl} = & 2\left(a - \frac{\lambda a_s}{u_s}\right) + \frac{1}{4\pi^2} \left\{ \frac{\lambda}{2} + \frac{S\hat{g}}{D_1} + 3\mathcal{C}[\beta_2\mathcal{D}_1 + (\beta_1 - \beta_2)\frac{\mathcal{D}_2}{D_1}] - \frac{2S^2\mathcal{E}_1\hat{g}}{D_1}\left(a - \frac{\lambda a_s}{u_s}\right) \right. \\ & - 6\mathcal{C}^2\left(a - \frac{\lambda a_s}{u_s}\right)[\beta_2\mathcal{D}_1^2 + (\beta_1 - \beta_2)\mathcal{D}_2] + a_s\lambda + \frac{4\mathcal{C}\mathcal{D}_1 a_s \lambda^2}{u_s} [1 - 2(\mathcal{C}\mathcal{D}_1\left(a - \frac{\lambda a_s}{u_s}\right) - a_s)] \\ & \left. - \frac{S\mathcal{F}^2\kappa^2}{8\mathcal{D}_1} [1 - 2(\mathcal{S}\mathcal{E}_1\left(a - \frac{\lambda a_s}{u_s}\right) - a_s)] \right\} + \left(\frac{\lambda}{u_s} \frac{da_s}{dl} + \frac{a_s}{u_s} \frac{d\lambda}{dl} - \frac{a_s\lambda}{u_s^2} \frac{du_s}{dl} \right), \end{aligned} \quad (22)$$

$$\begin{aligned} \frac{du_s}{dl} = & u_s + \frac{1}{2\pi^2} \left\{ -18a_s u_s^2 (1 + 6a_s) - \frac{16\mathcal{C}^3\mathcal{D}_1^3 a_s \lambda^3}{3u_s} [1 - 6\mathcal{C}\left(a - \frac{\lambda a_s}{u_s}\right)\mathcal{D}_1] - \frac{16\mathcal{S}^3\mathcal{E}_1^3 a_s \lambda^3}{3u_s} [1 - 6\mathcal{S}\left(a - \frac{\lambda a_s}{u_s}\right)\mathcal{E}_1] \right. \\ & + 8\lambda^2 (\mathcal{S}^3\mathcal{E}_1^3 + \mathcal{C}^3\mathcal{D}_1^3) \left(a - \frac{\lambda a_s}{u_s}\right) - 18a_s u_s^2 - \frac{9u_s^2}{2} - 2\lambda^2 (\mathcal{S}^2\mathcal{E}_1^2 + \mathcal{C}^2\mathcal{D}_1^2) - \frac{32\lambda_{\Delta A}^2}{3} \left(\frac{4\lambda_{\Delta A} a_s}{u_s} + 1\right) \\ & - \frac{11072a_s \lambda_{\Delta A}^3}{105u_s} \left(1 + \frac{6\lambda_{\Delta A} a_s}{u_s}\right) - \mathcal{C}\mathcal{S}\mathcal{F}^2\kappa^2 [1 - 2(\mathcal{C}\mathcal{D}_1 + \mathcal{S}\mathcal{E}_1)\left(a - \frac{\lambda a_s}{u_s}\right)] \\ & - \frac{\mathcal{C}^2\mathcal{S}^2\mathcal{F}^2 a_s^2 \kappa^2 (\mathcal{F}^2\kappa^2 + 2\mathcal{D}_1\mathcal{E}_1\lambda^2)}{6u_s^2} [1 - 4(\mathcal{C}\mathcal{D}_1 + \mathcal{S}\mathcal{E}_1)\left(a - \frac{\lambda a_s}{u_s}\right)] \\ & \left. - \frac{2\mathcal{C}^2\mathcal{S}\mathcal{F}^2\mathcal{D}_1 a_s \kappa^2 \lambda}{3u_s} [1 - 2(2\mathcal{C}\mathcal{D}_1 + \mathcal{S}\mathcal{E}_1)\left(a - \frac{\lambda a_s}{u_s}\right)] \right\}, \end{aligned} \quad (23)$$

$$\begin{aligned} \frac{d\lambda}{dl} = & \lambda + \frac{1}{2\pi^2} \left\{ \frac{-8\mathcal{S}^3\mathcal{E}_1^2 a_s \lambda^2 \hat{g}}{3\mathcal{D}_1 u_s} [1 - 6\mathcal{S}\mathcal{E}_1\left(a - \frac{\lambda a_s}{u_s}\right)] - \frac{8\mathcal{C}^3\mathcal{D}_1 a_s \lambda^2 [\beta_2\mathcal{D}_1^2 + (\beta_1 - \beta_2)\mathcal{D}_2]}{u_s} \right. \\ & \times [1 - 6\mathcal{C}\mathcal{D}_1\left(a - \frac{\lambda a_s}{u_s}\right)] - 4\mathcal{C}\mathcal{D}_1 a_s \lambda^2 [1 - 2(\mathcal{C}\mathcal{D}_1\left(a - \frac{\lambda a_s}{u_s}\right) - 2a_s)] - \frac{8\mathcal{C}^2\mathcal{D}_1^2 a_s \lambda^3}{3u_s} [1 - 2(2\mathcal{C}\mathcal{D}_1\left(a - \frac{\lambda a_s}{u_s}\right) - a_s)] \\ & + 3a_s u_s \lambda (1 + 6a_s) - \frac{S\mathcal{F}^2\kappa^2}{\mathcal{D}_1} [1 - 2(\mathcal{S}\mathcal{E}_1\left(a - \frac{\lambda a_s}{u_s}\right) - a_s)] + \frac{S^2\mathcal{E}_1\lambda\hat{g}}{\mathcal{D}_1} [4\mathcal{S}\mathcal{E}_1\left(a - \frac{\lambda a_s}{u_s}\right) - 1] \\ & - \frac{3u_s(1 + 4a_s)\lambda}{4} + 3\mathcal{C}^2\lambda[\beta_2\mathcal{D}_1^2 + (\beta_1 - \beta_2)\mathcal{D}_2][4\mathcal{C}\mathcal{D}_1\left(a - \frac{\lambda a_s}{u_s}\right) - 1] + 4\mathcal{C}\mathcal{D}_1\lambda^2 [2(\mathcal{C}\mathcal{D}_1\left(a - \frac{\lambda a_s}{u_s}\right) - a_s) - 1] \\ & - \frac{2\mathcal{S}^2\mathcal{F}^2\mathcal{E}_1\lambda a_s \kappa^2}{3\mathcal{D}_1 u_s} [1 - 2(2\mathcal{S}\mathcal{E}_1\left(a - \frac{\lambda a_s}{u_s}\right) - a_s)] - \frac{2\mathcal{C}\mathcal{S}\mathcal{F}^2 a_s \lambda \kappa^2}{3u_s} [1 - 2(\mathcal{C}\mathcal{D}_1 + \mathcal{S}\mathcal{E}_1)\left(a - \frac{\lambda a_s}{u_s}\right) + 2a_s] \\ & - \frac{\mathcal{C}^2\mathcal{S}^2\mathcal{E}_1\mathcal{F}^2\lambda a_s^2 \kappa^2 [\beta_2\mathcal{D}_1^2 + (\beta_1 - \beta_2)\mathcal{D}_2]}{2\mathcal{D}_1 u_s^2} [1 - 4(\mathcal{C}\mathcal{D}_1\left(a - \frac{\lambda a_s}{u_s}\right) + \mathcal{S}\mathcal{E}_1\left(a - \frac{\lambda a_s}{u_s}\right))] \\ & \left. - \frac{\mathcal{C}^2\mathcal{S}^2\mathcal{F}^2\lambda a_s^2 \kappa^2 \hat{g}}{6u_s^2} [1 - 4(\mathcal{C}\mathcal{D}_1 + \mathcal{S}\mathcal{E}_1)\left(a - \frac{\lambda a_s}{u_s}\right)] \right\}, \end{aligned} \quad (24)$$

$$\begin{aligned} \frac{d\beta_1}{dl} = & \frac{[(\mathcal{D}_1^2 - \mathcal{D}_2)\mathcal{E}_2 - (\mathcal{E}_1^2 - \mathcal{E}_2)\mathcal{D}_2]}{(\mathcal{D}_1^2\mathcal{E}_2 - \mathcal{E}_1^2\mathcal{D}_2)}\beta_1 + \frac{2(\mathcal{D}_1^2 - \mathcal{D}_2)}{2\pi^2(\mathcal{D}_1^2\mathcal{E}_2 - \mathcal{E}_1^2\mathcal{D}_2)} \left\{ \mathcal{C}^2\hat{g}^2 [4\mathcal{C}\mathcal{D}_1\left(a - \frac{\lambda a_s}{u_s}\right) - 1] \right. \\ & - \frac{\mathcal{E}_1^2\lambda^2(1 + 4a_s)}{4} - 9\mathcal{S}^2[\beta_2\mathcal{E}_1^2 + (\beta_1 - \beta_2)\mathcal{E}_2]^2 [1 - 4\mathcal{S}\mathcal{E}_1\left(a - \frac{\lambda a_s}{u_s}\right)] - \frac{4\mathcal{S}^2\mathcal{E}_1^2 a_s \lambda^2 [\beta_2\mathcal{E}_1^2 + (\beta_1 - \beta_2)\mathcal{E}_2]}{u_s} \\ & \times [1 - 2(2\mathcal{S}\mathcal{E}_1\left(a - \frac{\lambda a_s}{u_s}\right) - a_s)] - \frac{4\mathcal{S}\mathcal{E}_1^3 a_s \lambda^3}{3u_s} [1 - 2(\mathcal{S}\mathcal{E}_1\left(a - \frac{\lambda a_s}{u_s}\right) - 2a_s)] - \frac{2\mathcal{C}^2\mathcal{F}^2 a_s \kappa^2 \hat{g}}{3u_s} \\ & \times [1 - 2(2\mathcal{C}\mathcal{D}_1\left(a - \frac{\lambda a_s}{u_s}\right) - a_s)] \left. \right\} - \frac{2(\mathcal{E}_1^2 - \mathcal{E}_2)}{2\pi^2(\mathcal{D}_1^2\mathcal{E}_2 - \mathcal{E}_1^2\mathcal{D}_2)} \left\{ \frac{-4\mathcal{C}^2\mathcal{D}_1^2 a_s \lambda^2 [\beta_2\mathcal{D}_1^2 + (\beta_1 - \beta_2)\mathcal{D}_2]}{u_s} \right. \\ & \times [1 - 2(2\mathcal{C}\mathcal{D}_1\left(a - \frac{\lambda a_s}{u_s}\right) - a_s)] + 9\mathcal{C}^2[\beta_2\mathcal{D}_1^2 + (\beta_1 - \beta_2)\mathcal{D}_2]^2 [4\mathcal{C}\mathcal{D}_1\left(a - \frac{\lambda a_s}{u_s}\right) - 1] \\ & + \mathcal{S}^2\hat{g}^2 [4\mathcal{S}\mathcal{E}_1\left(a - \frac{\lambda a_s}{u_s}\right) - 1] - \frac{\mathcal{D}_1^2\lambda^2(1 + 4a_s)}{4} - \frac{4\mathcal{C}\mathcal{D}_1^3 a_s \lambda^3}{3u_s} [1 - 2(\mathcal{C}\mathcal{D}_1\left(a - \frac{\lambda a_s}{u_s}\right) - 2a_s)] \\ & \left. - \frac{2\mathcal{S}^2\mathcal{F}^2 a_s \kappa^2 \hat{g}}{3u_s} [1 - 2(2\mathcal{S}\mathcal{E}_1\left(a - \frac{\lambda a_s}{u_s}\right) - a_s)] \right\}, \end{aligned} \quad (25)$$

$$\begin{aligned} \frac{d\beta_2}{dl} = & \frac{(\mathcal{E}_2\mathcal{D}_1^2 - \mathcal{D}_2\mathcal{E}_1^2)}{(\mathcal{D}_1^2\mathcal{E}_2 - \mathcal{E}_1^2\mathcal{D}_2)}\beta_2 + \frac{2\mathcal{E}_2}{2\pi^2(\mathcal{D}_1^2\mathcal{E}_2 - \mathcal{E}_1^2\mathcal{D}_2)} \left\{ \mathcal{S}^2\hat{g}^2 [4\mathcal{S}\mathcal{E}_1\left(a - \frac{\lambda a_s}{u_s}\right) - 1] - \frac{\mathcal{D}_1^2\lambda^2(1 + 4a_s)}{4} \right. \\ & + 9\mathcal{C}^2[\beta_2\mathcal{D}_1^2 + (\beta_1 - \beta_2)\mathcal{D}_2]^2 [4\mathcal{C}\mathcal{D}_1\left(a - \frac{\lambda a_s}{u_s}\right) - 1] - \frac{4\mathcal{C}^2\mathcal{D}_1^2 a_s \lambda^2 [\beta_2\mathcal{D}_1^2 + (\beta_1 - \beta_2)\mathcal{D}_2]}{u_s} \\ & \times [1 - 2\left(2\mathcal{C}\mathcal{D}_1\left(a - \frac{\lambda a_s}{u_s}\right) - a_s\right)] - \frac{4\mathcal{C}\mathcal{D}_1^3 a_s \lambda^3}{3u_s} [1 - 2(\mathcal{C}\mathcal{D}_1\left(a - \frac{\lambda a_s}{u_s}\right) - 2a_s)] - \frac{2\mathcal{S}^2\mathcal{F}^2 a_s \kappa^2 \hat{g}}{3u_s} \\ & \times [1 - 2(2\mathcal{S}\mathcal{E}_1\left(a - \frac{\lambda a_s}{u_s}\right) - a_s)] \left. \right\} - \frac{2\mathcal{D}_2}{2\pi^2(\mathcal{D}_1^2\mathcal{E}_2 - \mathcal{E}_1^2\mathcal{D}_2)} \left\{ \frac{-4\mathcal{S}^2\mathcal{E}_1^2 a_s \lambda^2 [\beta_2\mathcal{E}_1^2 + (\beta_1 - \beta_2)\mathcal{E}_2]}{u_s} \right. \\ & \times [1 - 2(2\mathcal{S}\mathcal{E}_1\left(a - \frac{\lambda a_s}{u_s}\right) - a_s)] - 9\mathcal{S}^2[\beta_2\mathcal{E}_1^2 + (\beta_1 - \beta_2)\mathcal{E}_2]^2 [1 - 4\mathcal{S}\mathcal{E}_1\left(a - \frac{\lambda a_s}{u_s}\right)] + \mathcal{C}^2\hat{g}^2 \end{aligned}$$

$$\begin{aligned} & \times [4\mathcal{C}\mathcal{D}_1(a - \frac{\lambda a_s}{u_s}) - 1] - \frac{\mathcal{E}_1^2 \lambda^2 (1 + 4a_s)}{4} + \frac{-4\mathcal{S}\mathcal{E}_1^3 a_s \lambda^3}{3u_s} [1 - 2(\mathcal{S}\mathcal{E}_1(a - \frac{\lambda a_s}{u_s}) - 2a_s)] \\ & + \frac{-2\mathcal{C}^2 \mathcal{F}^2 a_s \kappa^2 \hat{g}}{3u_s} [1 - 2(2\mathcal{C}\mathcal{D}_1(a - \frac{\lambda a_s}{u_s}) - a_s)] \Big\}, \end{aligned} \quad (26)$$

$$\begin{aligned} \frac{d\lambda_{\Delta A}}{dl} = & \lambda_{\Delta A} + \frac{2}{2\pi^2} \left\{ \frac{-64a_s \lambda_{\Delta A}^3}{9u_s} [1 - 2(\mathcal{D}_1(a - \frac{\lambda a_s}{u_s}) - a_s)] - \frac{3a_s u_s \lambda_{\Delta A} (1 + 6a_s)}{2} - \frac{3u_s \lambda_{\Delta A} (4a_s + 1)}{8} \right. \\ & \left. - 4\lambda_{\Delta A}^2 [1 + 2a_s(1 + \frac{\lambda_{\Delta A}}{u_s})] - 4a_s \lambda_{\Delta A}^2 [1 + (4a_s + \frac{2\lambda_{\Delta A} a_s}{u_s})] \right\}, \end{aligned} \quad (27)$$

$$\begin{aligned} \frac{d\kappa}{dl} = & \kappa + \frac{2}{2\pi^2} \left\{ \frac{-2\mathcal{C}\mathcal{S}\mathcal{D}_1 \mathcal{E}_1 a_s \lambda^2 \kappa}{3u_s} [1 - 2(\mathcal{C}\mathcal{D}_1(a - \frac{\lambda a_s}{u_s}) + \mathcal{S}\mathcal{E}_1(a - \frac{\lambda a_s}{u_s}) - a_s)] - \frac{3a_s u_s \kappa (1 + 6a_s)}{2} \right. \\ & - \mathcal{C}\mathcal{S}\hat{g}\kappa [1 - 2(\mathcal{C}\mathcal{D}_1(a - \frac{\lambda a_s}{u_s}) + \mathcal{S}\mathcal{E}_1(a - \frac{\lambda a_s}{u_s}))] - \frac{3(1 + 4a_s)u_s \kappa}{8} - \frac{2\mathcal{C}\mathcal{S}^2 \mathcal{E}_1 \hat{g} a_s \kappa \lambda}{3u_s} \\ & \times [1 - 2(\mathcal{C}\mathcal{D}_1(a - \frac{\lambda a_s}{u_s}) + 2\mathcal{S}\mathcal{E}_1(a - \frac{\lambda a_s}{u_s}))] - \frac{\mathcal{C}^2 \mathcal{S}^2 \mathcal{F}^2 \hat{g} a_s^2 \kappa^3}{6u_s^2} [1 - 4(\mathcal{C}\mathcal{D}_1(a - \frac{\lambda a_s}{u_s}) + \mathcal{S}\mathcal{E}_1(a - \frac{\lambda a_s}{u_s}))] \\ & \left. - \frac{2\mathcal{C}^2 \mathcal{S}\mathcal{D}_1 \hat{g} a_s \kappa \lambda}{3u_s} [1 - 2(2\mathcal{C}\mathcal{D}_1(a - \frac{\lambda a_s}{u_s}) + \mathcal{S}\mathcal{E}_1(a - \frac{\lambda a_s}{u_s}))] \right\}, \end{aligned} \quad (28)$$

$$\begin{aligned} \frac{d\hat{g}}{dl} = & \hat{g} + \frac{1}{2\pi^2} \left\{ \frac{-4\mathcal{C}\mathcal{D}_1^2 \mathcal{E}_1 a_s \lambda^3}{3u_s} [1 - 2(\mathcal{C}\mathcal{D}_1(a - \frac{\lambda a_s}{u_s}) - 2a_s)] + \frac{-4\mathcal{S}\mathcal{D}_1 \mathcal{E}_1^2 a_s \lambda^3}{3u_s} [1 - 2(\mathcal{S}\mathcal{E}_1(a - \frac{\lambda a_s}{u_s}) - 2a_s)] \right. \\ & - \frac{32\mathcal{C}^2 \mathcal{D}_1^2 \hat{g} a_s \lambda^2}{3u_s} [1 - 2(2\mathcal{C}\mathcal{D}_1(a - \frac{\lambda a_s}{u_s}) - a_s)] + \mathcal{S}^3 \mathcal{E}_1(a - \frac{\lambda a_s}{u_s}) [\beta_2 \mathcal{E}_1^2 + (\beta_1 - \beta_2) \mathcal{E}_2] \\ & - \frac{32\mathcal{S}^2 \mathcal{E}_1^2 \hat{g} a_s \lambda^2}{3u_s} [1 - 2(2\mathcal{S}\mathcal{E}_1(a - \frac{\lambda a_s}{u_s}) - a_s)] - \frac{\mathcal{F}^2 (1 + 4a_s) \kappa^2}{4} - \frac{\mathcal{D}_1 \mathcal{E}_1 (4a_s + 1) \lambda^2}{4} \\ & + 12\hat{g} [\mathcal{C}^3 \mathcal{D}_1(a - \frac{\lambda a_s}{u_s}) [\beta_2 \mathcal{D}_1^2 + (\beta_1 - \beta_2) \mathcal{D}_2] + 8\mathcal{C}\mathcal{S}\hat{g}^2 [2(\mathcal{C}\mathcal{D}_1(a - \frac{\lambda a_s}{u_s}) \\ & + \mathcal{S}\mathcal{E}_1(a - \frac{\lambda a_s}{u_s})) - 1] - 3(\hat{g} - \beta_2 \mathcal{D}_1 \mathcal{E}_1) [\mathcal{C}^2 [\beta_2 \mathcal{D}_1^2 + (\beta_1 - \beta_2) \mathcal{D}_2] + \mathcal{S}^2 [\beta_2 \mathcal{E}_1^2 + (\beta_1 - \beta_2) \mathcal{E}_2]] \\ & - \frac{2\mathcal{C}^2 \mathcal{F}^2 [\beta_2 \mathcal{D}_1^2 + (\beta_1 - \beta_2) \mathcal{D}_2] a_s \kappa^2}{u_s} [1 - 2(2\mathcal{C}\mathcal{D}_1(a - \frac{\lambda a_s}{u_s}) - a_s)] - \frac{2\mathcal{S}^2 \mathcal{F}^2 [\beta_2 \mathcal{E}_1^2 + (\beta_1 - \beta_2) \mathcal{E}_2] a_s \kappa^2}{u_s} \\ & \times [1 - 2(2\mathcal{S}\mathcal{E}_1(a - \frac{\lambda a_s}{u_s}) - a_s)] - \frac{4\mathcal{C}^2 \mathcal{S}^2 \mathcal{F}^2 \hat{g}^2 a_s^2 \kappa^2}{3u_s^2} [1 - 4(\mathcal{C}\mathcal{D}_1(a - \frac{\lambda a_s}{u_s}) + \mathcal{S}\mathcal{E}_1(a - \frac{\lambda a_s}{u_s}))] \\ & - \frac{3\mathcal{C}^2 \mathcal{S}^2 \mathcal{F}^2 [\beta_2 \mathcal{D}_1^2 + (\beta_1 - \beta_2) \mathcal{D}_2] [\beta_2 \mathcal{E}_1^2 + (\beta_1 - \beta_2) \mathcal{E}_2] a_s^2 \kappa^2}{2u_s^2} [1 - 4(\mathcal{C}\mathcal{D}_1(a - \frac{\lambda a_s}{u_s}) + \mathcal{S}\mathcal{E}_1(a - \frac{\lambda a_s}{u_s}))] \\ & \left. - \frac{\mathcal{C}^2 \mathcal{S}^2 \mathcal{F}^2 \hat{g}^2 a_s^2 \kappa^2}{3u_s^2} [1 - 4(\mathcal{C}\mathcal{D}_1(a - \frac{\lambda a_s}{u_s}) + \mathcal{S}\mathcal{E}_1(a - \frac{\lambda a_s}{u_s}))] \right\}, \end{aligned} \quad (29)$$

where the variable functions are designated as

$$\mathcal{D}_1 \equiv |\mathbf{n}_X|^2 \cos^2 \theta, \quad \mathcal{D}_2 \equiv |\mathbf{n}_X^2|^2 \cos^4 \theta, \quad \mathcal{E}_1 \equiv |\mathbf{n}_Y|^2 \sin^2 \theta, \quad \mathcal{E}_2 \equiv |\mathbf{n}_Y^2|^2 \sin^4 \theta, \quad (30)$$

$$\mathcal{F} \equiv |\cos \theta \sin \theta \mathbf{n}_X \cdot \mathbf{n}_Y| + |\cos \theta \sin \theta \mathbf{n}_X \cdot \mathbf{n}_Y^*|, \quad \mathcal{C} \equiv 1/|\mathbf{n}_X \cos \theta|^2, \quad \mathcal{S} \equiv 1/|\mathbf{n}_Y \sin \theta|^2. \quad (31)$$

Here, we would like to stress that $\theta \in [0, \pi/2]$, and $\theta = 0, \pi/2$ serve as single magnetic order parameter with \mathbf{Q}_X or \mathbf{Q}_Y , respectively.

For type-II case, at which $|\mathbf{n}_i^2| \neq |\mathbf{n}_i|^4$ with $i = X, Y$, only one of β_1 and β_2 flows independently. In this circumstance, the flows of a_s , a , u_s , λ , $\lambda_{\Delta A}$ and κ share the same evolutions with their type-I counterparts. Nevertheless, the parameter \hat{g} evolves under the following way

$$\begin{aligned} \frac{d\hat{g}}{dl} = & \hat{g} + \frac{1}{2\pi^2} \left\{ \frac{-4\mathcal{C}\mathcal{D}_1^2 \mathcal{E}_1 a_s \lambda^3}{3u_s} [1 - 2(\mathcal{C}\mathcal{D}_1(a - \frac{\lambda a_s}{u_s}) - 2a_s)] - \frac{4\mathcal{S}\mathcal{D}_1 \mathcal{E}_1^2 a_s \lambda^3}{3u_s} [1 - 2(\mathcal{S}\mathcal{E}_1(a - \frac{\lambda a_s}{u_s}) - 2a_s)] \right. \\ & - \frac{32\mathcal{C}^2 \mathcal{D}_1^2 \hat{g} a_s \lambda^2}{3u_s} [1 - 2(2\mathcal{C}\mathcal{D}_1(a - \frac{\lambda a_s}{u_s}) - a_s)] - \frac{32\mathcal{S}^2 \mathcal{E}_1^2 \hat{g} a_s \lambda^2}{3u_s} [1 - 2(2\mathcal{S}\mathcal{E}_1(a - \frac{\lambda a_s}{u_s}) - a_s)] \\ & + 12\hat{g} [\mathcal{C}^3 \mathcal{D}_1(a - \frac{\lambda a_s}{u_s}) [\beta_2 \mathcal{D}_1^2 + (\beta_1 - \beta_2) \mathcal{D}_2] + \mathcal{S}^3 \mathcal{E}_1(a - \frac{\lambda a_s}{u_s}) [\beta_2 \mathcal{E}_1^2 + (\beta_1 - \beta_2) \mathcal{E}_2]] - \frac{\mathcal{D}_1 \mathcal{E}_1 (4a_s + 1) \lambda^2}{4} \\ & + 8\mathcal{C}\mathcal{S}\hat{g}^2 [2(\mathcal{C}\mathcal{D}_1(a - \frac{\lambda a_s}{u_s}) + \mathcal{S}\mathcal{E}_1(a - \frac{\lambda a_s}{u_s})) - 1] - \frac{\mathcal{F}^2 (1 + 4a_s) \kappa^2}{4} - 3\hat{g} [\mathcal{C}^2 [\beta_2 \mathcal{D}_1^2 + (\beta_1 - \beta_2) \mathcal{D}_2] \\ & + \mathcal{S}^2 [\beta_2 \mathcal{E}_1^2 + (\beta_1 - \beta_2) \mathcal{E}_2]] + \frac{-2\mathcal{C}^2 \mathcal{F}^2 [\beta_2 \mathcal{D}_1^2 + (\beta_1 - \beta_2) \mathcal{D}_2] a_s \kappa^2}{u_s} [1 - 2(2\mathcal{C}\mathcal{D}_1(a - \frac{\lambda a_s}{u_s}) - a_s)] \\ & \left. + \frac{-2\mathcal{S}^2 \mathcal{F}^2 [\beta_2 \mathcal{E}_1^2 + (\beta_1 - \beta_2) \mathcal{E}_2] a_s \kappa^2}{u_s} [1 - 2(2\mathcal{S}\mathcal{E}_1(a - \frac{\lambda a_s}{u_s}) - a_s)] - \frac{4\mathcal{C}^2 \mathcal{S}^2 \mathcal{F}^2 \hat{g}^2 a_s^2 \kappa^2}{3u_s^2} \right\} \end{aligned}$$

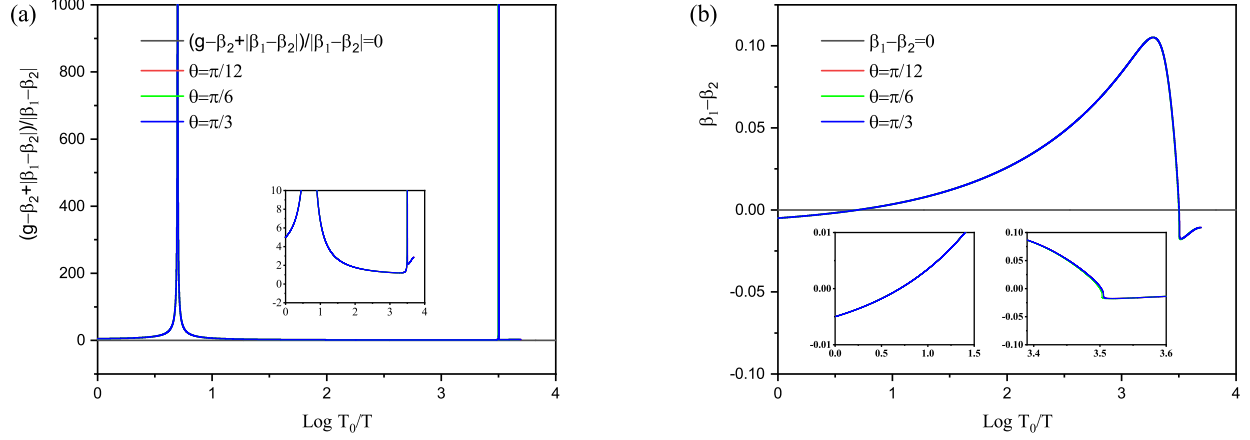


FIG. 4: (Color online) Temperature-dependent stable constraints of C_2 -symmetry ICS under representative starting values of interaction parameters (the qualitative results are insensitive to initial values of parameters): (a) $(g - \beta_2 + |\beta_1 - \beta_2|)/|\beta_1 - \beta_2|$ and (b) $\beta_1 - \beta_2$. Insets: sign-change region of $\beta_1 - \beta_2$ (left panel) and (b) behaviors around l_c (right panel).

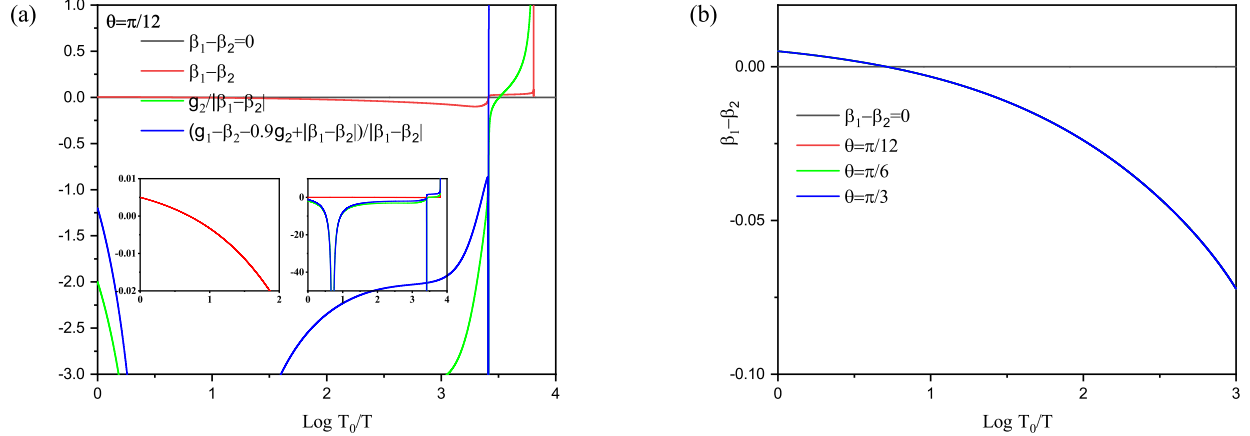


FIG. 5: (Color online) (a) Temperature-dependent stable constraints of C_2 -symmetry DPMH under representative starting values of interaction parameters (the qualitative results are insensitive to the initial values). Insets: sign-change region of $\beta_1 - \beta_2$ (left panel) and enlarged-region for $\frac{g-\tilde{\beta}}{|\beta-\tilde{\beta}|} - \frac{g}{10} \frac{\tilde{g}}{|\beta-\tilde{\beta}|} + 1$ (right panel). (b) Sign-change regions of $\beta_1 - \beta_2$ under different values of θ .

$$\begin{aligned}
& \times [1 - 4(\mathcal{CD}_1(a - \frac{\lambda a_s}{u_s}) + \mathcal{SE}_1(a - \frac{\lambda a_s}{u_s}))] - \frac{3\mathcal{C}^2 \mathcal{S}^2 \mathcal{F}^2 [\beta_2 \mathcal{D}_1^2 + (\beta_1 - \beta_2) \mathcal{D}_2] [\beta_2 \mathcal{E}_1^2 + (\beta_1 - \beta_2) \mathcal{E}_2] a_s^2 \kappa^2}{2u_s^2} \\
& \times [1 - 4(\mathcal{CD}_1(a - \frac{\lambda a_s}{u_s}) + \mathcal{SE}_1(a - \frac{\lambda a_s}{u_s}))] - \frac{\mathcal{C}^2 \mathcal{S}^2 \mathcal{F}^2 \hat{g}^2 a_s^2 \kappa^2}{3u_s^2} [1 - 4(\mathcal{CD}_1(a - \frac{\lambda a_s}{u_s}) + \mathcal{SE}_1(a - \frac{\lambda a_s}{u_s}))]. \quad (32)
\end{aligned}$$

Furthermore, the RG equations of parameters β_1 and β_2 can be broken down into six distinct sorts depending on the concrete conditions.

For type-II case-A with $|\mathbf{n}_X^2|^2 = |\mathbf{n}_X|^4$, $|\mathbf{n}_Y^2|^2 = |\mathbf{n}_Y|^4$, $|\mathbf{n}_Z^2|^2 = 0$ and $|\mathbf{n}_X^2|^2 \neq 0$, β_1 evolves but β_2 is an invariant constant,

$$\begin{aligned}
\frac{d\beta_1}{dl} &= \beta_1 + \frac{2}{2\pi^2} \left\{ \frac{-4\mathcal{C}^2 \mathcal{D}_1^2 a_s \lambda^2 \beta_1}{u_s} [1 - 2(2\mathcal{CD}_1(a - \frac{\lambda a_s}{u_s}) - a_s)] + 9\mathcal{C}^2 \mathcal{D}_2 \beta_1^2 [4\mathcal{CD}_1(a - \frac{\lambda a_s}{u_s}) - 1] - \frac{\lambda^2 (1 + 4a_s)}{4} \right. \\
& \left. + \frac{\mathcal{S}^2 \hat{g}^2}{\mathcal{D}_2} [4\mathcal{SE}_1(a - \frac{\lambda a_s}{u_s}) - 1] - \frac{4\mathcal{CD}_1 a_s \lambda^3}{3u_s} [1 - 2(\mathcal{CD}_1(a - \frac{\lambda a_s}{u_s}) - 2a_s)] \right\}
\end{aligned}$$

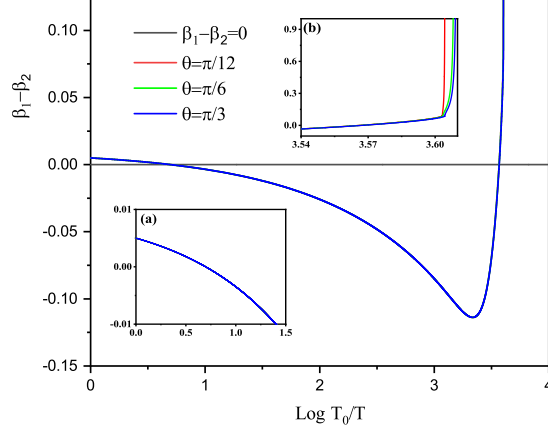


FIG. 6: (Color online) Temperature-dependent stable constraints $(\beta_1 - \beta_2)$ of C_2 -symmetry MH under representative starting values of interaction parameters (the qualitative results are insensitive to the initial values). Insets: (a) sign-change region of $\beta_1 - \beta_2$ and (b) behaviors around l_c .

$$-\frac{2\mathcal{S}^2\mathcal{F}^2 a_s \kappa^2 \hat{g}}{3\mathcal{D}_2 u_s} \left[1 - 2(2\mathcal{S}\mathcal{E}_1(a - \frac{\lambda a_s}{u_s}) - a_s) \right], \quad (33)$$

$$\frac{d\beta_2}{dl} = 0. \quad (34)$$

For type-II case-B with $|\mathbf{n}_X^2|^2 = |\mathbf{n}_X|^4$, $|\mathbf{n}_Y^2|^2 = |\mathbf{n}_Y|^4$, $|\mathbf{n}_X^2|^2 = 0$ and $|\mathbf{n}_Y^2|^2 \neq 0$, β_1 evolves whereas β_2 is an invariant constant,

$$\begin{aligned} \frac{d\beta_1}{dl} = & \beta_1 + \frac{2}{2\pi^2} \left\{ \frac{-4\mathcal{S}^2\mathcal{E}_1^2 a_s \lambda^2 \beta_1}{u_s} [1 - 2(2\mathcal{S}\mathcal{E}_1(a - \frac{\lambda a_s}{u_s}) - a_s)] - 9\mathcal{S}^2\mathcal{E}_2\beta_1^2 [1 - 4\mathcal{S}\mathcal{E}_1(a - \frac{\lambda a_s}{u_s})] - \frac{\lambda^2(1 + 4a_s)}{4} \right. \\ & + \frac{\mathcal{C}^2 \hat{g}^2}{\mathcal{E}_2} [4\mathcal{C}\mathcal{D}_1(a - \frac{\lambda a_s}{u_s}) - 1] - \frac{4\mathcal{S}\mathcal{E}_1 a_s \lambda^3}{3u_s} [1 - 2(\mathcal{S}\mathcal{E}_1(a - \frac{\lambda a_s}{u_s}) - 2a_s)] \\ & \left. - \frac{2\mathcal{C}^2\mathcal{F}^2 a_s \kappa^2 \hat{g}}{3\mathcal{E}_2 u_s} [1 - 2(2\mathcal{C}\mathcal{D}_1(a - \frac{\lambda a_s}{u_s}) - a_s)] \right\}, \end{aligned} \quad (35)$$

$$\frac{d\beta_2}{dl} = 0. \quad (36)$$

For type-II case-C with $|\mathbf{n}_X^2|^2 = |\mathbf{n}_X|^4$, $|\mathbf{n}_Y^2|^2 \neq |\mathbf{n}_Y|^4$, $|\mathbf{n}_Y^2|^2 = 0$, and $|\mathbf{n}_X^2|^2 = 0$, β_2 evolves but β_1 is an invariant constant,

$$\frac{d\beta_1}{dl} = 0, \quad (37)$$

$$\begin{aligned} \frac{d\beta_2}{dl} = & \beta_2 + \frac{2}{2\pi^2} \left\{ \frac{-4\mathcal{S}^2 a_s \lambda^2 [\beta_2 \mathcal{E}_1^2 + (\beta_1 - \beta_2) \mathcal{E}_2]}{u_s} [1 - 2(2\mathcal{S}\mathcal{E}_1(a - \frac{\lambda a_s}{u_s}) - a_s)] - 9\mathcal{S}^2 \beta_2^2 \mathcal{E}_1^2 [1 - 4\mathcal{S}\mathcal{E}_1(a - \frac{\lambda a_s}{u_s})] \right. \\ & + \frac{\mathcal{C}^2 \hat{g}^2}{\mathcal{E}_1^2} [4\mathcal{C}\mathcal{D}_1(a - \frac{\lambda a_s}{u_s}) - 1] - \frac{4\mathcal{S}\mathcal{E}_1 a_s \lambda^3}{3u_s} [1 - 2(\mathcal{S}\mathcal{E}_1(a - \frac{\lambda a_s}{u_s}) - 2a_s)] - \frac{\lambda^2(1 + 4a_s)}{4} \\ & \left. - \frac{2\mathcal{C}^2\mathcal{F}^2 a_s \kappa^2 \hat{g}}{3\mathcal{E}_1^2 u_s} [1 - 2(2\mathcal{C}\mathcal{D}_1(a - \frac{\lambda a_s}{u_s}) - a_s)] \right\}. \end{aligned} \quad (38)$$

For type-II case-D with $|\mathbf{n}_Y^2|^2 = |\mathbf{n}_Y|^4$, $|\mathbf{n}_X^2|^2 \neq |\mathbf{n}_X|^4$, $|\mathbf{n}_Y^2|^2 = 0$, and $|\mathbf{n}_X^2|^2 = 0$, β_2 evolves but β_1 is an invariant constant,

$$\frac{d\beta_1}{dl} = 0, \quad (39)$$

$$\begin{aligned} \frac{d\beta_2}{dl} = & \beta_2 + \frac{2}{2\pi^2} \left\{ \frac{-4\mathcal{C}^2 a_s \lambda^2 [\beta_2 \mathcal{D}_1^2 + (\beta_1 - \beta_2) \mathcal{D}_2]}{u_s} [1 - 2(2\mathcal{C}\mathcal{D}_1(a - \frac{\lambda a_s}{u_s}) - a_s)] + 9\mathcal{C}^2 \beta_2^2 \mathcal{D}_1^2 [4\mathcal{C}\mathcal{D}_1(a - \frac{\lambda a_s}{u_s}) - 1] \right. \\ & \left. + \frac{\mathcal{S}^2 \hat{g}^2}{\mathcal{D}_1^2} [4\mathcal{S}\mathcal{E}_1(a - \frac{\lambda a_s}{u_s}) - 1] - \frac{\lambda^2(1 + 4a_s)}{4} - \frac{4\mathcal{C}\mathcal{D}_1 a_s \lambda^3}{3u_s} [1 - 2(\mathcal{C}\mathcal{D}_1(a - \frac{\lambda a_s}{u_s}) - 2a_s)] \right\} \end{aligned}$$

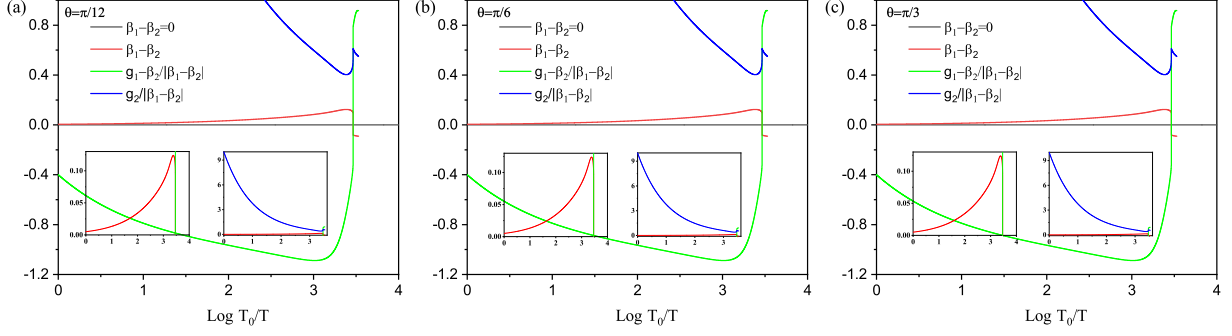


FIG. 7: (Color online) Temperature-dependent stable constraints of C_2 -symmetry ICS \perp MH under representative starting values of interaction parameters (the qualitative results are insensitive to the initial values): (a) $\theta = \pi/12$, (b) $\theta = \pi/6$, and (c) $\theta = \pi/3$. Insets: enlarged regions for $\beta_1 - \beta_2$ (left panel) and $g_2/|\beta_1 - \beta_2|$ (right panel).

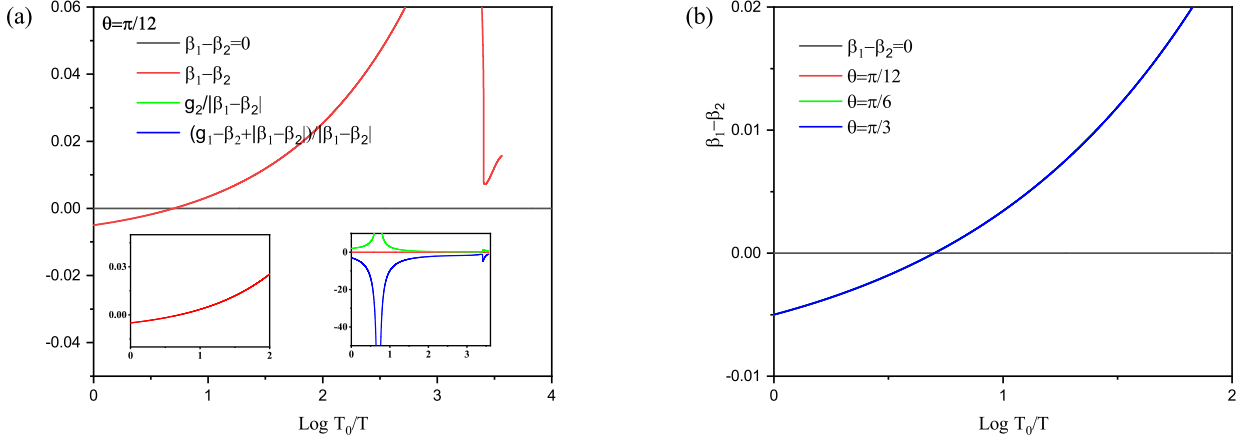


FIG. 8: (Color online) (a) Temperature-dependent stable constraints of C_4 -symmetry SVC under representative starting values of interaction parameters (the qualitative results are insensitive to initial values of parameters). Inset: enlarge region for $g_2/|\beta_1 - \beta_2|$ and $(g_1 + |\beta_1 - \beta_2|)/|\beta_1 - \beta_2|$. (b) Sign-change regions at different values of θ .

$$-\frac{2\mathcal{S}^2\mathcal{F}^2 a_s \kappa^2 \hat{g}}{3\mathcal{D}_1^2 u_s} \left[1 - 2(2\mathcal{S}\mathcal{E}_1(a - \frac{\lambda a_s}{u_s}) - a_s) \right] \}. \quad (40)$$

For type-II case-E with $|\mathbf{n}_Y^2| \neq |\mathbf{n}_Y|^4$, $|\mathbf{n}_X^2| \neq |\mathbf{n}_X|^4$, $|\mathbf{n}_Y^2| = 0$, and $|\mathbf{n}_X^2| = 0$, β_2 evolves but β_1 is an invariant constant,

$$\frac{d\beta_1}{dl} = 0, \quad (41)$$

$$\begin{aligned} \frac{d\beta_2}{dl} = & \beta_2 + \frac{2}{2\pi^2} \left\{ \frac{-4\mathcal{C}^2 a_s \lambda^2 [\beta_2 \mathcal{D}_1^2 + (\beta_1 - \beta_2) \mathcal{D}_2]}{u_s} [1 - 2(2\mathcal{C}\mathcal{D}_1(a - \frac{\lambda a_s}{u_s}) - a_s)] + 9\mathcal{C}^2 \beta_2^2 \mathcal{D}_1^2 [4\mathcal{C}\mathcal{D}_1(a - \frac{\lambda a_s}{u_s}) - 1] \right. \\ & + \frac{\mathcal{S}^2 \hat{g}^2}{\mathcal{D}_1^2} [4\mathcal{S}\mathcal{E}_1(a - \frac{\lambda a_s}{u_s}) - 1] - \frac{\lambda^2 (1 + 4a_s)}{4} - \frac{4\mathcal{C}\mathcal{D}_1 a_s \lambda^3}{3u_s} [1 - 2(\mathcal{C}\mathcal{D}_1(a - \frac{\lambda a_s}{u_s}) - 2a_s)] \\ & \left. - \frac{2\mathcal{S}^2 \mathcal{F}^2 a_s \kappa^2 \hat{g}}{3\mathcal{D}_1^2 u_s} [1 - 2(2\mathcal{S}\mathcal{E}_1(a - \frac{\lambda a_s}{u_s}) - a_s)] \right\}. \end{aligned} \quad (42)$$

For type-II case-F with $\mathcal{E}_2 \mathcal{D}_1^2 - \mathcal{D}_2 \mathcal{E}_1^2 = 0$, both β_1 and β_2 are energy-independent constants,

$$\frac{d\beta_1}{dl} = 0, \quad \frac{d\beta_2}{dl} = 0. \quad (43)$$

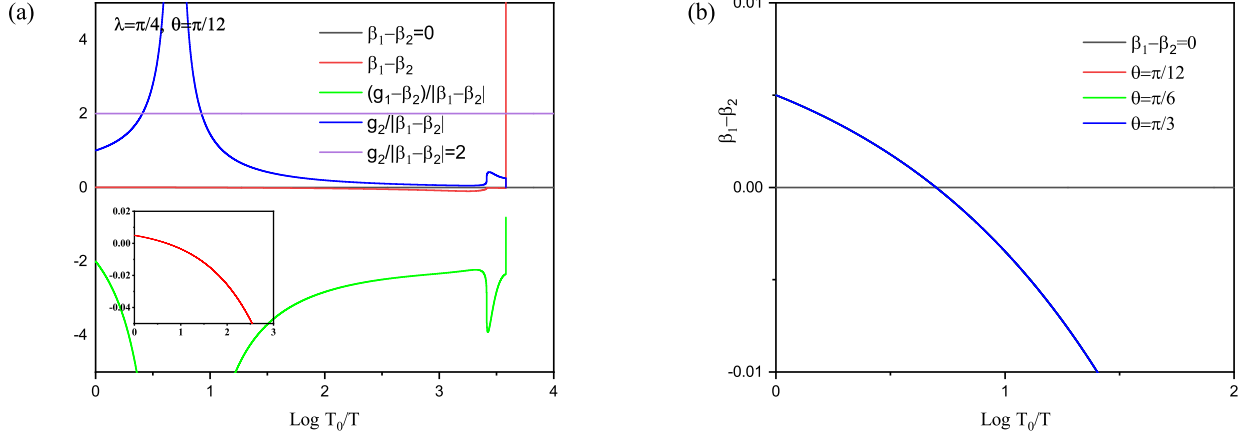


FIG. 9: (Color online) (a) Temperature-dependent stable constraints of symmetric double- \mathbf{Q} noncoplanar SWC under representative starting values of interaction parameters (the qualitative results are insensitive to initial values of parameters). Inset: enlarge region for $\beta_1 - \beta_2$. (b) Sign-change regions at different values of θ .

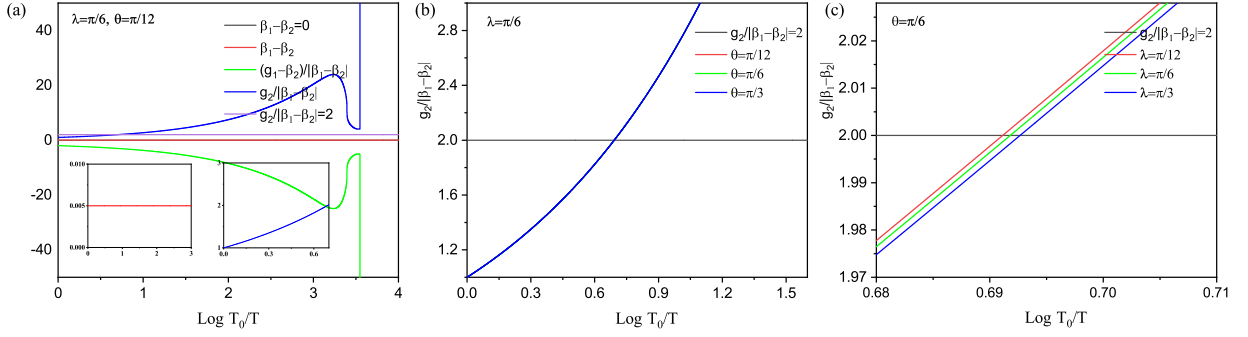


FIG. 10: (Color online) (a) Temperature-dependent stable constraints of asymmetric double- \mathbf{Q} noncoplanar SWC under representative starting values of interaction parameters (the qualitative results are insensitive to initial values of parameters). Inset: enlarge region for $\beta_1 - \beta_2$. (b) and (c) Sign-change regions at different values of θ and λ .

STABILITIES OF INCOMMENSURATE MAGNETIC STATES

As aforementioned in the maintext, there are seven different types of incommensurate (IC) magnetic states other than three commensurate ones including stripe spin density wave (SDW), charge spin density wave (CSDW), and spin vortex crystal (SVC) [16, 17, 34, 35]. To be concrete, these IC magnetic states cover four different C_2 -symmetry (C_2) IC cases consisting of C_2 IC stripe (ICS), C_2 magnetic helix (MH), C_2 IC magnetic stripe with perpendicular magnetic helix (ICS \perp MH), and C_2 double parallel magnetic helix (DPMH), as well as three distinct C_4 -symmetry (C_4) IC situations involving C_4 IC CSDW, C_4 IC SVC, and C_4 IC spin-whirl crystal (SWC) [19]. In order to examine whether these IC magnetic states are stable against the decrease of energy scales, we within this section lean upon the coupled RG equations (21)-

(43), which are completely encoded with the information of ordering competition, in conjunction with their stable constraints catalogued in Table I of the maintext.

In principle, the energy variable of RG evolution is expressed by $\Lambda = \Lambda_0 e^{-l}$ with $l > 0$ denoting the running scale. As our study is concerned with the structure of schematic phase diagram, it is herein of remarkable convenience to associate l with temperature via designating $T = T_0 e^{-l}$ with T_0 being the initial temperature to measure the evolution of energy scale [18, 32]. On the basis of this transformation and RG equations, we are now in a proper position to judge whether these IC magnets are good candidates residing in the phase diagram of $\text{Ba}_{1-x}\text{Na}_x\text{Fe}_2\text{As}_2$ one by one.

We start out by considering the C_2 IC magnetic states. On one hand, the configurations of spin vectors for C_2 ICS magnetic state read $\mathbf{n}_X = (0, 0, 1)$ and $\mathbf{n}_Y = (0, 0, 0)$ [19], which satisfy the restricted conditions

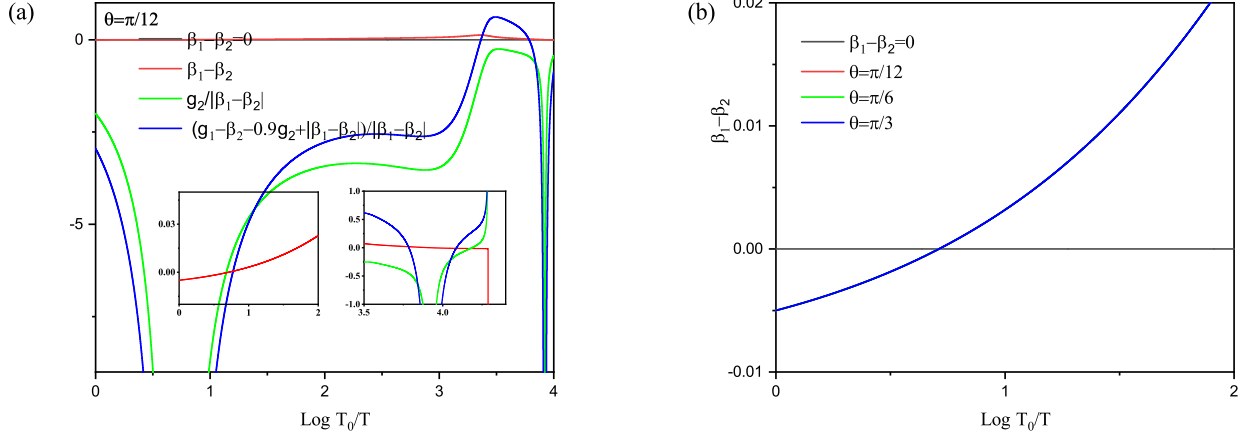


FIG. 11: (Color online) (a) Temperature-dependent stable constraints C_4 -symmetry IC CSDW for case-1 under representative starting values of interaction parameters (the qualitative results are insensitive to initial values of parameters). Inset: sign-change region of $(g_2 + |\beta_1 - \beta_2|)/|\beta_1 - \beta_2|$. (b) Sign-change regions at different values of θ .

of type-II case-A. This indicates the interaction parameters obey the RG evolutions of type-II case-A delineated in Eqs. (21)-(24), (27), (28), and (32)-(34). As for C_2 ICS, its stable constraints can be either $(\beta_1 - \beta_2) < 0$, $g_2/|\beta_1 - \beta_2| > 0$, $(g_1 - \beta_2)/|\beta_1 - \beta_2| > -1$ or $(\beta_1 - \beta_2) < 0$, $g_2/|\beta_1 - \beta_2| < 0$, $(g_1 - \beta_2 - 0.9g_2)/|\beta_1 - \beta_2| > -1$ [19]. Based on these, we perform numerical RG analysis by taking some initial representative values of parameters and obtain the results shown in Fig. 4. On the other, concerning C_2 MH and C_2 DPMH, the configurations of spin vectors are characterized by $\mathbf{n}_X = \frac{1}{\sqrt{2}}(i, 0, 1)/$, $\mathbf{n}_Y = (0, 0, 0)$, and $\mathbf{n}_X = \frac{1}{\sqrt{2}}(i, 0, 1)$, $\mathbf{n}_Y = \frac{1}{\sqrt{2}}(i, 0, 1)$, respectively [19]. Accordingly, this indicates that the interaction parameters are dictated by the evolutions for type-II case-D provided in Eqs. (21)-(24), (27), (28), (32), and (39)-(40). To proceed, we parallel the analogous RG numerical analysis taking advantage of the corresponding constraints [19] $(\beta_1 - \beta_2) > 0$, $g_2/|\beta_1 - \beta_2| > 0$, $(g_1 - \beta_2)/|\beta_1 - \beta_2| > 0$ or $(\beta_1 - \beta_2) > 0$, $g_2/|\beta_1 - \beta_2| < 0$, $(g_1 - \beta_2 - 0.9g_2)/|\beta_1 - \beta_2| > -1$ for C_2 MH and $(\beta_1 - \beta_2) > 0$, $g_2/|\beta_1 - \beta_2| < 0$, $(g_1 - \beta_2 - 0.9g_2)/|\beta_1 - \beta_2| < -1$ for C_2 DPMH, respectively. The conclusions are underscored in Fig. 5 and Fig. 6 with taking some representative beginning values of parameters. Learning from Fig. 4, Fig. 5, and Fig. 6, we apparently figure out that the sign change of $\beta_1 - \beta_2$ is occurred explicitly once temperature is slightly lowered owing to the effects of ordering competition. As a consequence, we infer that C_2 ICS, C_2 MH and C_2 DPMH are not stable states in the low-energy regime and hence not good candidates for IC magnetic state nearby the QCP in phase diagram of $\text{Ba}_{1-x}\text{Na}_x\text{Fe}_2\text{As}_2$. However, these three C_2 IC states might be suitable states for the quantum critical region with high temperatures, such as C_2 IC SDW illustrated

in Fig. 1.

In a sharp contrast, with respect to C_2 ICS \perp MH, whose the configurations of spin vectors are related to $\mathbf{n}_X = (0, 0, 1)$ and $\mathbf{n}_Y = \frac{1}{\sqrt{2}}(i, 1, 0)$ [19], their interaction parameters are therefore subject to type-I coupled RG equations (21)-(29). Carrying out the similar numerical analysis gives rise to temperature-dependent evolutions depicted in Fig. 7. It manifestly heralds that stable constraints of C_2 ICS \perp MH, i.e., $(\beta_1 - \beta_2) > 0$, $(g_1 - \beta_2)/|\beta_1 - \beta_2| < 0$, and $g_2/|\beta_1 - \beta_2| > f(g_1 - \beta_2) \approx 2$ for a finite value of $g_1 - \beta_2$ and $\lim_{(g_1 - \beta_2) \rightarrow 0} f(g_1 - \beta_2) \rightarrow 0$ [19], are remarkably robust against ordering competition as the temperature is decreased. Despite of relative stability, it is very necessary to point out that C_2 ICS \perp MH can be destroyed as long as the magnetic QCP is closely accessed, at which the ordering competition becomes so ferocious that any state cannot present solely.

Next, we go to judge C_4 IC magnetic states, which include C_4 IC SVC, C_4 SWC, and C_4 IC CSDW. In analogy to C_2 IC magnetic states, we inspect low-energy fates of these states by combining their RG equations and stable constraints. For C_4 IC SVC with the configurations of spin vectors being $\mathbf{n}_X = (0, 0, 1)$ and $\mathbf{n}_Y = (0, 1, 0)$ [19], the interaction parameters are governed by the type-II case-A RG equations (21)-(24), (27), (28), (32)-(34) and the stable constraints correspond to $(\beta_1 - \beta_2) < 0$, $g_2/|\beta_1 - \beta_2| > 0$, and $(g_1 - \beta_2)/|\beta_1 - \beta_2| < -1$ [19]. The numerical results presented in Fig. 8 reflect that C_4 IC SVC cannot be a well stable state in the phase diagram caused by the influence of ordering competition.

To proceed, we turn to C_4 IC SWC, which is well protected by constraints $(\beta_1 - \beta_2) > 0$, $(g_1 - \beta_2)/|\beta_1 - \beta_2| < 0$, and $0 < g_2/|\beta_1 - \beta_2| < 2$ [19]. In addition, the configurations of spin vectors are equivalent to $\mathbf{n}_X = (i \cos \phi, 0, \sin \phi)$ and $\mathbf{n}_Y = (0, i \cos \phi, \sin \phi)$. Be-

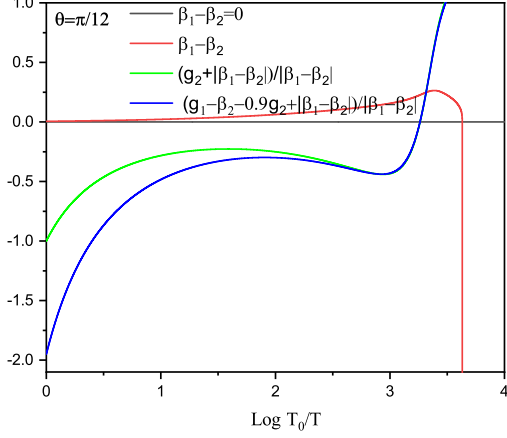
of $\text{Ba}_{1-x}\text{Na}_x\text{Fe}_2\text{As}_2$.

FIG. 12: (Color online) Temperature-dependent stable constraints C_4 -symmetry IC CSDW for case-2 under representative starting values of interaction parameters (the qualitative results are insensitive to initial values of parameters).

fore going further, it is of particular interest to address that they can be clustered into two sub-situations distinguished by the parameter ϕ which characterize the symmetric double- \mathbf{Q} noncoplanar SWC with $\phi = \pi/4$ and asymmetric double- \mathbf{Q} noncoplanar with $\phi \neq \pi/4$, respectively [19]. As a result, the former interaction parameters are dictated by type-II case-A RG equations (21)-(24), (27), (28), and (32)-(34) but instead the latter ones evolve under type-II case-F RG equations exhibited in Eqs. (21)-(24), (27), (28), (32), and (43). Carrying out analogous RG steps yields to Fig. 9 and Fig. 10, which explicitly signals C_4 SWC is not suitable to be present in the phase diagram.

Further, we move to C_4 IC CSDW state, at which the configurations of spin vectors are of the form $\mathbf{n}_X = (0, 0, 1)$ and $\mathbf{n}_Y = (0, 0, 1)$ [19], and thus type-II case-A RG equations (21)-(24), (27), (28), and (32)-(34) are in charge of the low-energy fates of interaction parameters. Hereby, it is necessary to highlight that C_4 -symmetry IC CSDW [19] can be stabilized by either $(\beta_1 - \beta_2) < 0, g_2/|\beta_1 - \beta_2| < 0, (g_1 - \beta_2 - 0.9g_2)/|\beta_1 - \beta_2| < -1$ (case-1) or $(\beta_1 - \beta_2) > 0, g_2/|\beta_1 - \beta_2| < -1, (g_1 - \beta_2 - 0.9g_2)/|\beta_1 - \beta_1| < -1$ (case-2). Fig. 11 and Fig. 12 collect the central results stemming from RG analysis, which manifestly exhibit the temperature (energy) dependence of associated parameters for C_4 IC CSDW. In the light of these figures, we are informed that stable constraints for both case-1 and case-2 are considerably robust with the decrease of temperature, which of course can be sabotaged due to sufficiently strong fluctuations so long as the magnetic QCP is closely approached. Consequently, C_4 IC CSDW, like its C_2 ICS \perp MH counterpart, is of fair robustness against ordering competition and an appropriate candidate for C_4 magnetic state in phase diagram